

Solid sorbent direct air capture using geothermal energy resources (S-DAC-GT) – Region specific analysis

Timur Kuru, Keivan Khaleghi, Silviu Livescu *

University of Texas at Austin, United States



ABSTRACT

This paper reviews the potential use of low temperature geothermal resources for thermal energy necessary for CO₂ direct air capture (DAC) processes (geothermal DAC or S-DAC-GT). The paper includes a literature review of DAC processes and existing techno-economic analyses on the subject. It also provides a list of global geothermal resources, maps, and databases that would be useful in finding areas of high favorability for S-DAC-GT deployment across the world. Finally, it concludes with a techno-economic analysis of four specific regions within the United States and one European region that may potentially be attractive S-DAC-GT sites: Texas Gulf Coast, Los Angeles Basin, Alaska's Cook Inlet, and Netherlands Groningen Gas Field.

The objective of this paper is to provide region specific techno-economic analyses of DAC using geothermal resources. Existing DAC techno-economic analyses of DAC are region agnostic and include a breadth of energy sources. This paper provides a deeper technical and economic analysis using geothermal energy as the thermal resource for the DAC process, and the results of this paper differentiate S-DAC-GT costs and carbon intensity by region.

There remains a substantial amount of uncertainty in forecasting DAC costs when deployed at scale. The goal of this paper is not to determine a precise S-DAC-GT cost. Rather, our goal is to provide indicative savings from using geothermal resources coupled with DAC, and to provide relative S-DAC-GT costs by region.

Reflecting the uncertainty around the cost of DAC, our analysis suggests a S-DAC-GT cost range of \$200 to \$1040 per tonne CO₂ captured, depending on the underlying cost model and the region of the S-DAC-GT facility. However, the savings calculated from using geothermal resources to provide the thermal energy are more consistent (Figure 1).

We also analyze the relative carbon intensity of S-DAC-GT within each region. In our model, we rely on geothermal resources to provide only thermal energy for the DAC regenerative process. The carbon intensity of S-DAC-GT by region is captured in Figure 2.

1. Introduction

Direct air capture (DAC) can play an important role in the net zero future. CO₂ can be captured directly from the air, in locations independent of the emitting sources, and be permanently stored in subsurface formations or used as a climate-neutral feedstock. Thus, the great advantage of DAC is that it can provide a solution for reducing or balancing emissions from sources that are difficult to avoid, such as heavy industry and existing transportation, as well as for removing emissions already in the air. DAC technologies are predicted to capture more than 85 Mt of CO₂ in 2030 and around 980 Mt CO₂ in 2050, requiring a fast accelerated scale-up from the 18 small-scale facilities operating today in Canada, EU, and the US (IEA, 2022a). To put these numbers in perspective, the first large-scale DAC plant to capture 1 Mt CO₂/year is expected to start operating in the US in a couple of years (OFX, 2022).

Today, DAC costs are the highest among all CO₂ capturing technologies. The CO₂ in the air is much more dilute than in, for example, flue gas from a power plant or a cement plant, contributing to DAC's higher

energy needs relative to the other CO₂ capturing applications. However, with innovation and technology deployment, DAC's capturing costs could significantly fall to under USD 100/t CO₂ by 2030 (IEA, 2022a). DAC costs are dependent on the capturing technology, heat and electricity costs, and other specific plant configuration and economic assumptions. IEA estimates that, with strong public and private support for innovation and technology deployment, the least cost locations for DAC development could be in the Middle East, China, EU, North Africa, and the US.

The two main types of DAC technologies used today are solid sorbent DAC (S-DAC), which requires relatively low temperatures (~100 °C) to release captured CO₂, and aqueous solvent DAC (L-DAC), which require temperatures as high as 900 °C to release captured CO₂. S-DAC can be combined with renewable energy sources, including heat pumps and geothermal, whereas L-DAC relies on natural gas for heat, as it requires very high temperatures. Coupling S-DAC with direct heat from geothermal wells (S-DAC-GT) could potentially reach the billion-tonne scale of removal necessary for capturing millions of tonnes of CO₂ per year (McQueen et al., 2020). For instance, there are many places around

* Corresponding author.

E-mail address: silviu.livescu@gmail.com (S. Livescu).

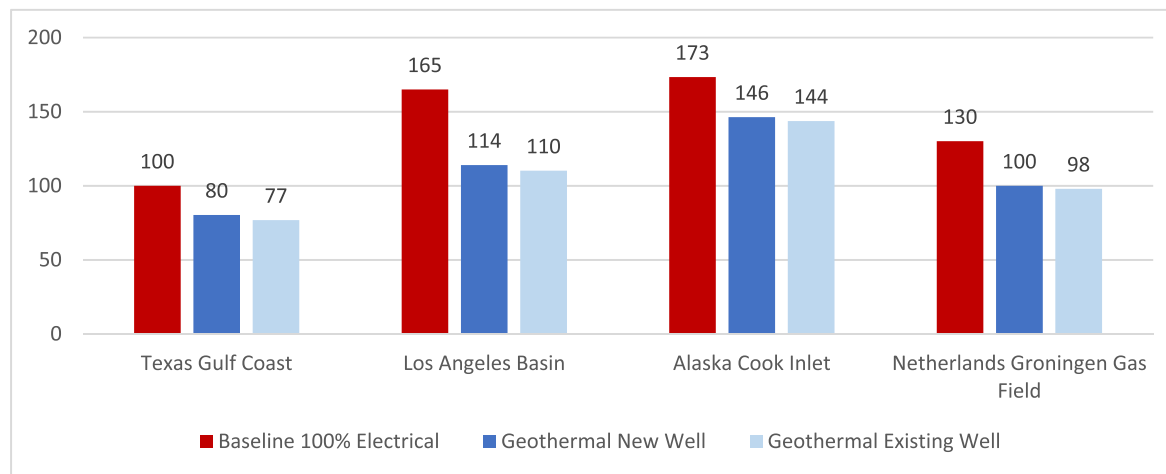


Fig. 1. Normalized cost of DAC per tonne CO₂ captured.

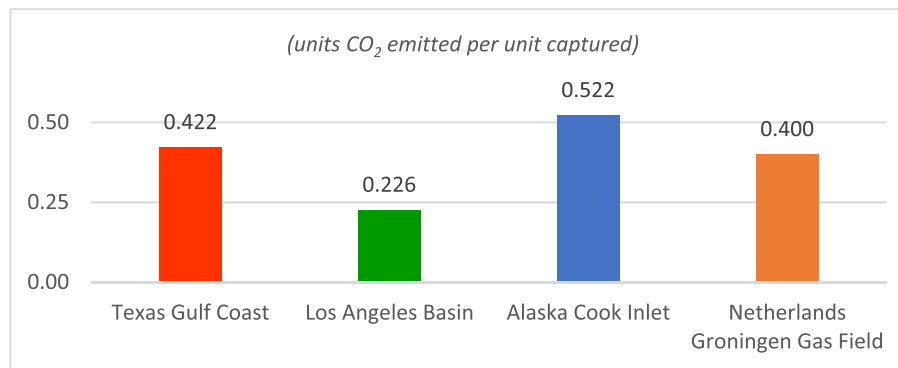


Fig. 2. Carbon intensity of S-DAC-GT.

the world where brines with temperatures of 80–120 °C can be produced with the current oil and gas technologies (Geothermal Technologies, 2019). This temperature range could be used for S-DAC, which is based on solid sorbents operating through an adsorption/desorption cycling process. While the adsorption takes place at ambient temperature and pressure, the desorption happens at low pressure and temperatures of ~100 °C. Currently, geothermal resources with brines at 80–120 °C are under-utilized or otherwise mostly used for power generation. The conversion from thermal energy to electrical power has an average global efficiency of 12% (Sadiq, 2014), meaning that most of the geothermal energy brought to surface is lost during conversion. Using these low-temperature geothermal resources for direct heat applications, such as S-DAC, instead of for power generation, would significantly increase their value while helping reduce S-DAC costs.

While a major advantage of DAC is that, theoretically, a DAC plant can be located anywhere, in reality, its location and cost would depend on the availability of low carbon intensity energy and a CO₂ storage resource or CO₂ use opportunity. A comprehensive study for evaluating the techno-economic potential of combining S-DAC and geothermal energy and identifying potential gaps and opportunities for scale-up is discussed below.

Our analysis shows that S-DAC-GT could provide a range of 16% to 33% (average 23%) cost reduction relative to a baseline model DAC facility. The averages of the models by region indicate that the Texas Gulf Coast would be the lowest cost S-DAC-GT region, while Alaska's Cook Inlet would be the most expensive. Fig. 1 shows the cost range of DAC in different regions, using different sources of thermal energy, normalized for a Texas Gulf Coast baseline facility relying 100% on regional electricity for thermal energy.

We also analyze the relative carbon intensity of S-DAC-GT within each region. S-DAC also requires considerable electric energy to power air blowers, compression, and other auxiliary systems. The carbon intensity of regional S-DAC-GT will, therefore, primarily depend on the profile of the energy sources for regional electricity. Our results indicate that the Los Angeles Basin would have the lowest carbon intensity, consistent with California's electricity infrastructure which relies on a higher share of renewable sources. The carbon intensity of S-DAC-GT by region is captured in Fig. 2.

2. Literature review

This literature review intends to compile scholarly research and data that are applicable to completing region-specific techno-economic analyses of DAC using geothermal resources. This review includes a) an introduction to DAC technology, b) a review of recent techno-economic analyses, c) geothermal gradient data from existing oil and gas wells that could be repurposed to provide the necessary thermal energy for DAC, and d) a brief overview of potential sites for geological CO₂ storage within the United States.

2.1. Introduction to DAC technology

The two leading DAC technologies are solid DAC (S-DAC) and liquid DAC (L-DAC). S-DAC has lower temperature requirements compared with L-DAC (100 °C versus 900 °C). On the other hand, S-DAC is more energy intensive vs L-DAC (7.2–9.5 GJ/tCO₂ vs 5.5–8.8 GJ/tCO₂) (IEA, 2022a). The lower temperature requirement makes geothermal direct use and geothermal heat pumps feasible options to supply the process

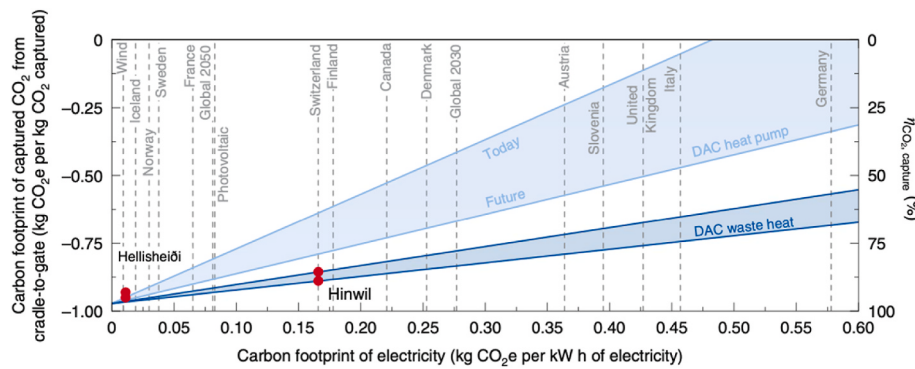


Fig. 3. Lifecycle carbon footprint of Climeworks DAC operations (Deutz and Bardow, 2021).

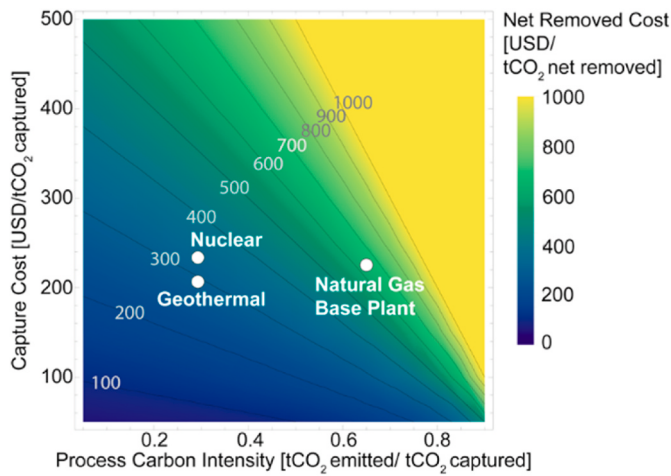


Fig. 4. Comparison of capture cost (McQueen et al., 2020).

heat for S-DAC while further lowering the carbon footprint of the DAC unit which in turn increases the overall carbon removal efficiency. In S-DAC, the solid adsorbents capture the CO₂ at ambient conditions and then release it during a desorption cycle occurring at temperatures around 80–120 °C and moderate vacuum pressures (200–1000 millibar_{abs}). An alternative to the temperature-swing regeneration method, is a moisture swing approach where moisturizing the sorbents releases the CO₂ (Fasihi et al., 2019). A number of commercial solid sorbents processes are being pursued.

S-DAC performance may be influenced by the climate of the capture site. In dry climates, the produced water, which is a side product of the process, can be produced and re-used; but, in humid climates, planning for the profuse amounts of produced water is needed. On the other hand, the increased CO₂ uptake capacity of the sorbent material in the presence of water and the dilution of CO₂ and the corresponding decrease of

Table 1

Parameters influencing the performance of S-DAC systems (Sinha and Realff, 2019)-(A) and (Nat. Acad. of Sci, Eng., and Med. (2019)- (B).

Parameter	Units	Range (A)	Range (B)
Inputs			
Contactor to adsorbent ratio	kg/kg	0.10–4.0	0.10–4.0
Adsorbent purchase cost	\$/kg	15–100	15–100
Adsorbent lifetime	year	NA	0.25–5.0
Sorbent total capacity (at 400 ppm)	mol/kg	0.5–1.5	0.5–1.5
Desorption swing capacity	mol/mol	0.75–0.90	0.75–0.90
CO ₂ to water ratio		0.025–0.5	NA
Air velocity	m/s	1–5	1–5
Desorption pressure (VSA)	bar	0.2–1.0	0.2–1.0
Desorption final temperature (TSA)	K	340–373	340–373
Heat of adsorption (CO ₂)	kJ/mol	40–90	40–90
Outputs			
Adsorption time	min	8–50	8–50
Desorption	min	7–35	7–35
Mass transfer coefficient	1/s	0.01–0.1	0.01–0.1
Pressure drop	Pa	300–1400	300–1400

its partial pressure by water results in higher CO₂ adsorption capacity. Also in humid conditions, the sorbents are less prone to degradation caused by O₂ (Wurzbacher et al., 2016). Overall, it is advantageous that the water consumption of this technology is negative considering the water scarcity issues across the world and especially in its dry regions (IEA, 2022a).

Deutz and Bardow (2021) reported the life-cycle carbon footprint of a geothermal powered DAC plant in Hellisheiði to be close to –1.00. The projected removal efficiency in several European countries and Canada are reported with heat provided via a heat pump system (coefficient of performance = 2.51) or waste heat streams, see Fig. 3. McQueen et al. (2020) compared the performance of natural gas (base case), geothermal (waste thermal energy of a geothermal powerplant) and nuclear energy (waste heat stream) sources coupled with solid DAC. Geothermal and nuclear sources lower the carbon footprint of the

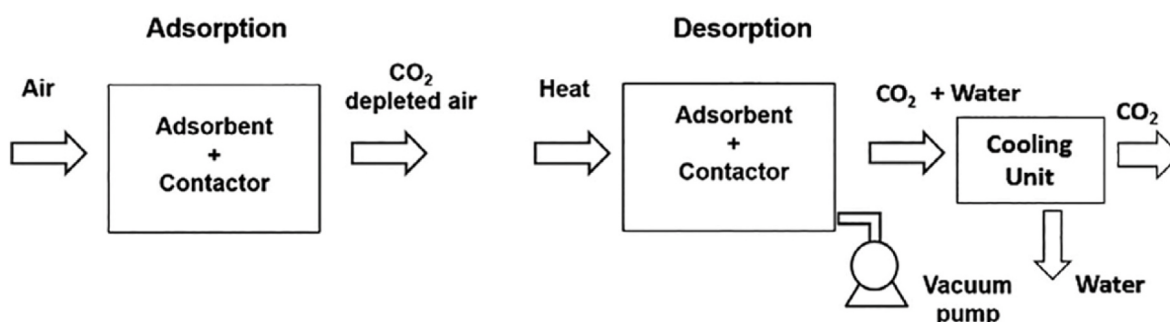


Fig. 5. Schematic of S-DAC process (Sinha and Realff, 2019).

Table 2

Estimated energy requirements for S-DAC systems – (Sinha and Realff, 2019).

Type	Energy Required (GJ/tCO ₂)		
	C:A ^a = 4:1	C:A = 1:1	C:A = 0.1:1
Thermal Energy	4.60–19.30	3.50–9.16	1.85–6.50
Electrical Energy	0.12–3.79	0.09–2.46	0.08–2.03
Cost (\$/tCO ₂)	18–1030	14–1015	14–1065

^a C:A = contactor to adsorbent ratio.**Table 3**Estimated costs for a 1 M/year CO₂ S-DAC system Nat. Acad. of Sci, Eng., and Med (2019).

Energy Source		Capture Cost (\$/tCO ₂)	
Electric	Thermal	Captured	Net Removed
solar	solar	88–228	89–256
nuclear	nuclear	88–228	89–250
solar	NG	88–228	113–326
wind	NG	88–228	113–326
NG	NG	88–228	124–407
coal	coal	88–228	166–877

Table 5

Estimated energy requirements for S-DAC systems (Nat. Acad. of Sci, Eng., and Med. (2019)).

Step	Type	Energy Required (GJ/tCO ₂)	
		Mid-Range (2–4)	Full-Range (1–5)
Desorption heat (100 °C sat steam)	Thermal	3.4–4.8	1.85–19.3
Air contactor fans	Electrical	0.55–1.12	0.08–3.79
Desorption vacuum pump	Electrical	(110–140) × 10 ⁻⁴	(4–910) × 10 ⁻⁴
Total		3.95–5.92	1.93–23.09

capture process, reducing the carbon intensity from 0.65 to 0.29 tCO₂/emitted/tCO₂, captured, this also meaningfully decreases the cost of capture, see Fig. 4.

Solid sorbent systems consist of two processes: adsorption and desorption. Solid sorbents within an air contactor absorb the CO₂ in the air and then exposure to heat and/or vacuum results in the liberation of CO₂, see Fig. 5.

2.2. Techno-economic analysis for DAC process

We will review the existing literature on techno-economic feasibility of S-DAC-GT process. Sinha and Realff (2019) and a report by National Academy of Science, Engineering and Medicine (2019) estimated the energy intensities of S-DAC by varying a number of process parameters, the models parameters and outputs are presented in Table 1, Table 2 and Table 3.

As it can be seen, the range of input for both models are identical. In (Sinha and Realff, 2019), wide ranges of removal cost for CO₂ are estimated. The reason is the importance of the mass ratio of contactor to adsorbents parameter on the overall cost of the process. High values of this parameter might result in high thermal loads for the contactor and low values might cause mechanical stability issues. Energy requirements

and removals costs for this model are presented in Table 2.

The report by National Academies of Sciences, Engineering, and Medicine introduces a cost analysis of capture via S-DAC systems. The results are presented in Table 5.

It is evident from Table 4 and Fig. 6 that the highest uncertainty is introduced by the adsorbent CAPEX. And except for scenario 1, adsorbent CAPEX incurs the highest percentage of the total costs.

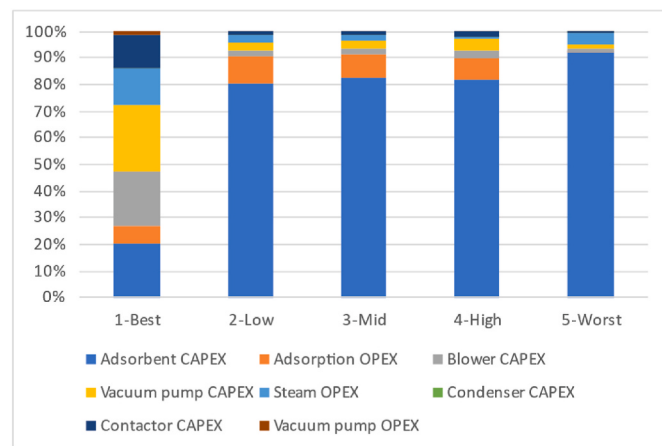
Another economic analysis of S-DAC unit is performed by (Fasihi et al., 2019). Levelized cost of DAC (LCOD) is calculated based on thermal and electrical demands of the process. The model parameters and estimated removal cost are presented in the following table.

McQueen et al. (2020) compared the cost of DAC coupled to three different low-carbon thermal energy sources: 1- steam generated by natural gas combustion (base case), 2- Waste heat of geothermal powerplant and 3- steam generated in a nuclear powerplant. The authors only considered already existing geothermal powerplants in the United States. Because of corrosion and scaling effects of geothermal fluids, the capital expense for the heat exchanger was tripled and this caused the geothermal option to have a higher capital cost compared to the base case. On the other hand, eliminating the operating costs due to steam, meaningfully lowered the geothermal operating costs, see Fig. 7. It should be highlighted that this scheme is considering geothermal electrical power as the source to generate the process heat and is essentially different from the scheme under consideration in this paper.

Valentine et al. (2022) performed a cost analysis on the DAC process.

Table 4Estimated capital and operating costs (annualized) of 1 Mt/y CO₂ S-DAC (Nat. Acad. of Sci, Eng., and Med (2019)).

Parameters	1-Best	2-Low	3-Mid	4-High	5-Worst
Adsorbent CAPEX	3.6	70	122	186	988
Adsorption OPEX	1.3	9	12	19	4.3
Blower CAPEX	3.6	2.1	3.7	6.7	13.7
Vacuum pump CAPEX	4.5	2.6	4.7	8.5	17.4
Steam OPEX	2.5	2.2	2.4	3	43
Condenser CAPEX	0.03	0.07	0.075	0.1	0.4
Contactor CAPEX	2.2	1.3	2.3	4.1	8.4
Vacuum pump OPEX	0.3	0.2	0.2	0.24	0.3

**Fig. 6.** Cost breakdown based on the data in Table 5.**Table 6**

Economics of solid-DAC unit (Fasihi et al., 2019).

Parameters	Capacity	Capex	Opex	El. Demand	Th. Demand	Cost
Unit Value	tonneCO ₂ /year 360,000	€/tonneCO ₂ -year 730	% 4	kWh _{el} /tonne 250	kWh _{th} /tonne 1750	€/tonneCO ₂ 155/120 ^a

^a Based on free waste heat.

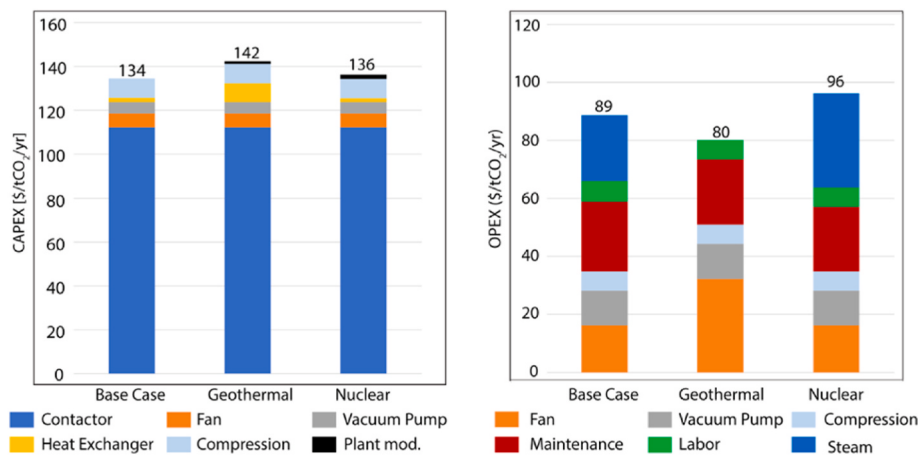


Fig. 7. Estimated capital and operating costs (annualized) (McQueen et al., 2020).

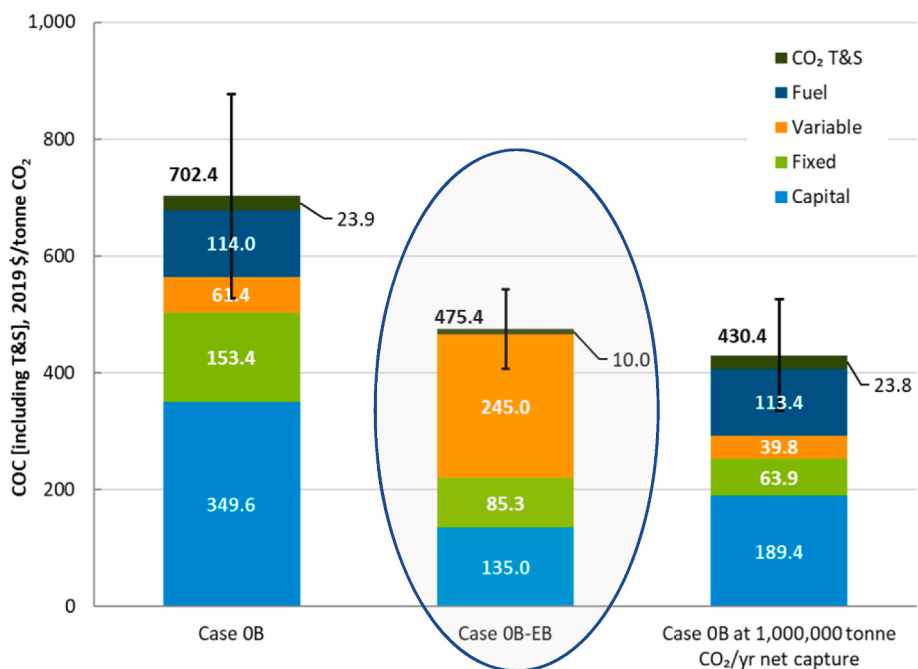


Fig. 8. Cost of carbon capture according to (Valentine et al., 2022).

They considered scenarios with different sources of heat for adsorbent regeneration. Of interest to this work, is the Case 0 B-EB in which an electric boiler is set to generate the steam needed for regeneration. This study assumes that the process used to produce the purchased electricity does not emit any CO₂, see Fig. 8.

In this section, the S-DAC process was introduced and briefly reviewed. We also surveyed the existing literature on the economic analysis of S-DAC process especially coupled with renewable/less carbon intensive sources of energy. The techno-economic assessment in this paper builds upon the references reviewed in this section.

2.3. Oil and Gas Well Data and Co-produced Resources in Regions of Interest

Using data from oil and gas wells to map the geothermal potential of a region has been crucial to lay the foundation for development and growth of geothermal industry in the coming decades. Converting abandoned oil and gas wells to geothermal wells is under consideration.

Moreover, harvesting energy in thermal and electrical forms from

brines co-produced along oil and gas is garnering attention in recent years and is an area of active research and commercial exploration. In this section, we review the existing literature with data relevant to regions of interest to this study.

Peterson (2013) reviewed the data of 1160 wells in the Cook Inlet in Alaska. 998 wells included bottomhole temperature (BHT) measurements and 226 had drill stem test fluid temperature (DST). The BHT measurements needed correction as the BHT data was obtained after drilling. The author calculated the thermal gradient to be in the range of 0.95–1.83 °F/100 ft. It is noteworthy that proximity to the active faults correlated with higher geothermal gradients. No flow rate data was provided. See Fig. 9.

Glassley et al. (2013) investigated the oil pools in the Los Angeles Basin (see Table 6). The focus of their study was geothermal power generation through a binary powerplant thus they chose 91 °C as a cut-off temperature to assess the suitability of the resources for power production, see Fig. 10 and Table 7.

The Texas Gulf Coast region seems like a suitable candidate for potential S-DAC-GT complexes. The temperature maps presented by

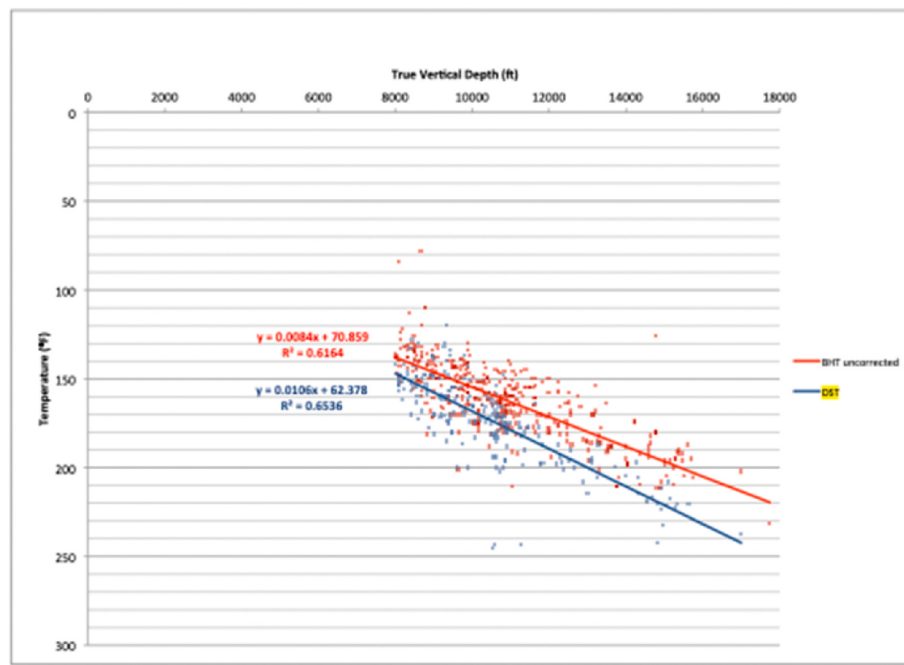


Fig. 9. Bottomhole temperature data for wells in the Cook Inlet, Alaska (Peterson, 2013).

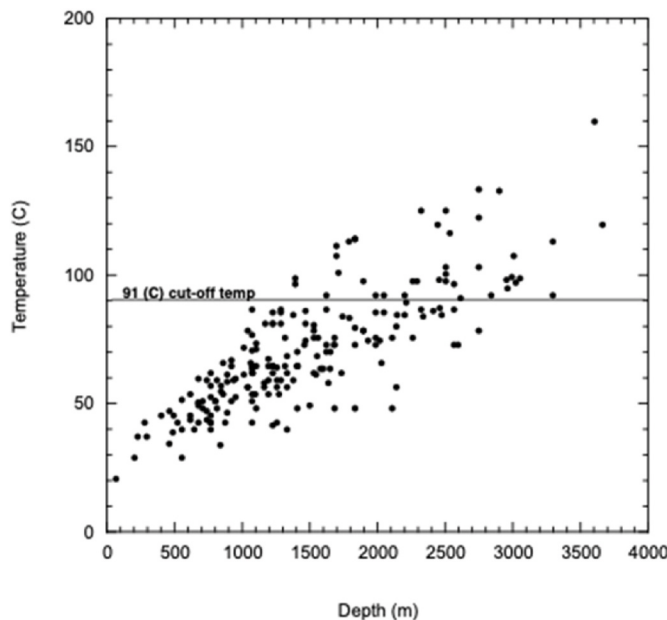


Fig. 10. Temperature versus depth data for oil pools in the Los Angeles Basin (Glassley et al., 2013).

(Zafar, 2023) based on existing well data illustrate suitable temperatures for S-DAC thermal requirements, see Fig. 11 (see Fig. 12). Table 8

Another location under consideration in this study is northern Netherlands. Bonté et al. (2012) presented a dataset for the country with an average thermal gradient of 31.3 °C/km, see Fig. 13. They also used a finite volume approximation to generate a 3D subsurface temperature map for the country.

2.4. Storage of CO₂

The section offers a brief overview on subsurface storage of CO₂. Fig. 14 illustrates the sedimentary basins in the United States

Table 7
Oil pools in Los Angeles Basin with geothermal potential (Glassley et al., 2013).

Name	Min. Temp. (°C)	Max. Temp (°C)	Geopressured	Substation (km)
Castaic Junction	97	120	Y	
Newhall Potrero	76	160	Y/N	
Sawtelle		133	N	1.0
Alondra		134	N	0.5
Inglewood	37	101	N	0
Seal Beach (S. Blk.)	64	125	Y	0
Seal Beach (Marine)	73	98	N	0
Santa Fe Springs	54	103	N	0
Oak Canyon	55	100	N	
Beverly Hills	86	103	N	0.5
East				
Long Beach (Old Area)	44	92	Y/N	0
Playa del Rey		98	N	1.0
Wilmington (On Shore)	51	113	N	0
Rosecrans	84	98	N	0
Seal Beach (N. Blk.)	51	92	N	0

superimposed on CO₂ emission sources. Of note is the presence of sedimentary basins in Texas Gulf Coast and Southern California suitable for carbon storage. Additional details such as CO₂ pipelines and potential sources of thermal energy can be found in Fig. 15.

3. Geothermal maps & databases

One of the major geothermal databases in the United States is the Department of Energy's Geothermal Data Repository - GDR (Weers et al., 2022). The database serves a number of purposes: storage of public data easily accessible by the geothermal scientific community and an integrated part of the project management system by the DOE Geothermal Technologies Office. The metadata is shared with a number of partner websites which makes the available data easily discoverable, see Fig. 16 for more details.

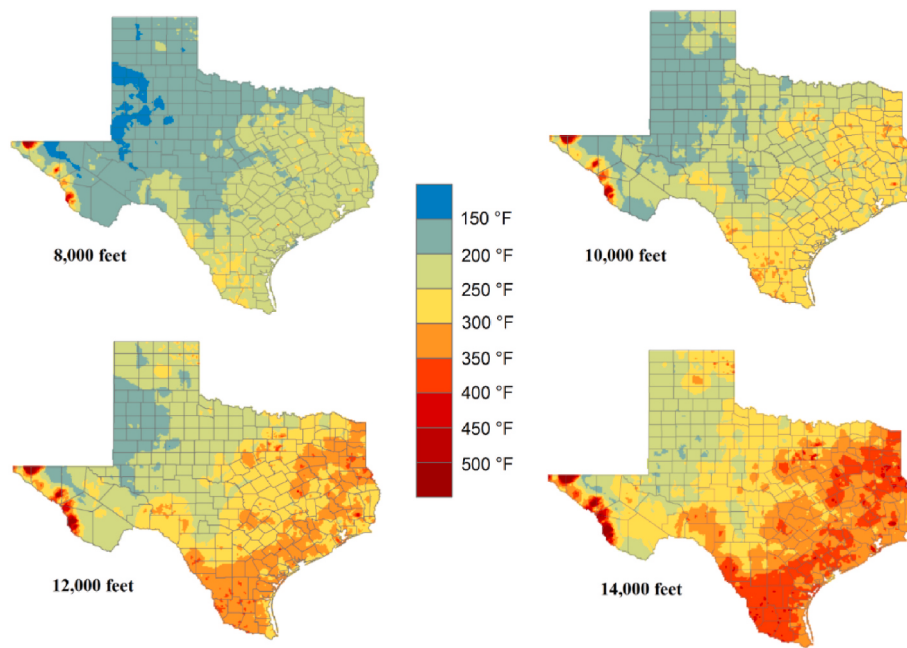


Fig. 11. Subsurface temperature in the state of Texas (Zafar, 2023)

More specifically counties such as Chambers, Galveston and Harris in the Texas Gulf Coast region show favorable temperatures for direct heat applications such as S-DAC-GT.

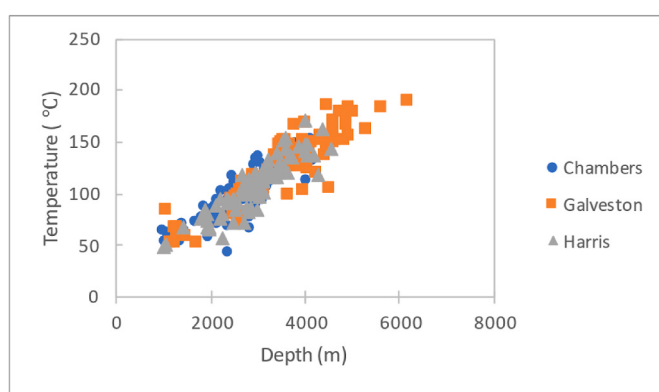


Fig. 12. Bottomhole temperatures in three Gulf Coast counties (Geology) Augustine and Falkenstern (2013) studied the potential of co-produced water from active oil and gas wells in the United states to generate electricity. is included to summarize their findings.

Table 8

Volume of co-produced water in three states: Alaska, California and Texas (Augustine and Falkenstern, 2013).

State	Active Wells	Co-produced Water Volume (bbl/year)	
		Total	Estimated Temp >176 °F (80 °C)
AK	2309	740,218,875	NA
CA	52,055	2,653,300,165	74,753,706
TX	63,542	2,607,232,920	2,199,237,843

Overall, there is ample evidence that geothermal resources suitable for S-DAC exist in three areas of interest in the US: Texas Gulf Coast, Alaska's Cook Inlet, and the Los Angeles Basin.

To assess the geothermal potential of a particular location, bottom-hole temperature, and heat flow data are needed. Heat flow is calculated as the multiplication of thermal conductivity and temperature gradient. In this section, we review existing databases and useful maps for North

America and other notable parts of the world. It is noteworthy that the list of top 10 countries in the world in terms of installed geothermal power, versus direct use applications (included in Table 9), have a few names in common. This indicates the fundamental difference in the way geothermal energy is utilized in its different forms.

A pioneering contribution by the American Association of Petroleum Geologists (AAPG) and US Geological Survey (USGS) was the subsurface temperature, geothermal gradient, and heat flow maps of North America (Fig. 17). As the data for these maps were sourced from different measurement types (drilling, etc.) and geographical regions, the different corrections factors applied may have introduced certain inaccuracies. Also, gradient values more than two standard deviations from the mean were excluded, and this may lead to failure in detecting geothermal anomalies (Vaught, 1980).

Blackwell and Richards (2023) at Southern Methodist University (SMU) built on the AAPG map and other data to construct a more complete and updated map of temperature and heat flow for North America (Fig. 18).

An updated version of the map by the SMU team offered a revised heat flow map based on 35,000 data sites (Blackwell et al., 2011). In addition to using more data points to produce the map, a number of other improvements are implemented including increasing the accuracy of bottomhole temperature measurements including additional calibration wells and thermal conductivity model of the overlaying sedimentary sections (Fig. 19).

Recently, machine learning methods have been employed to assess geothermal favorability. For example, a team at US geological survey, employed three modern machine learning algorithms (logistic regression, support vector machines, and XGBoost) to produce favorability maps for geothermal resources in the western United States (Mordensky et al., 2022). Fig. 20 was generated using a web tool made available by USGS (Western United States Geothermal Favorability | U.S. Geological Survey).

Batir et al. (2013) offered a heat flow map of Alaska (Fig. 21). This map was further expanded and updated, see (Batir et al., 2016).

For a comprehensive database on oil and gas and geothermal wells in the state of California, utilize the well finder and other GIS data (CA Department of Conservation - Well Finder Tool). For the state of Texas, the

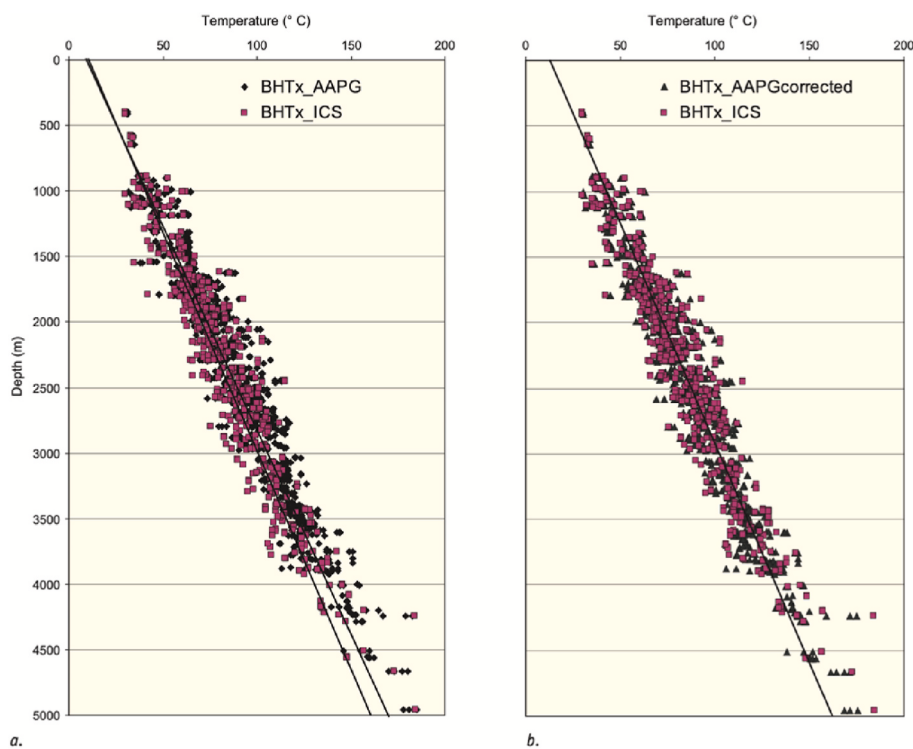


Fig. 13. Calculated geothermal gradient for the Netherlands based on two methods (Bonté et al., 2012).

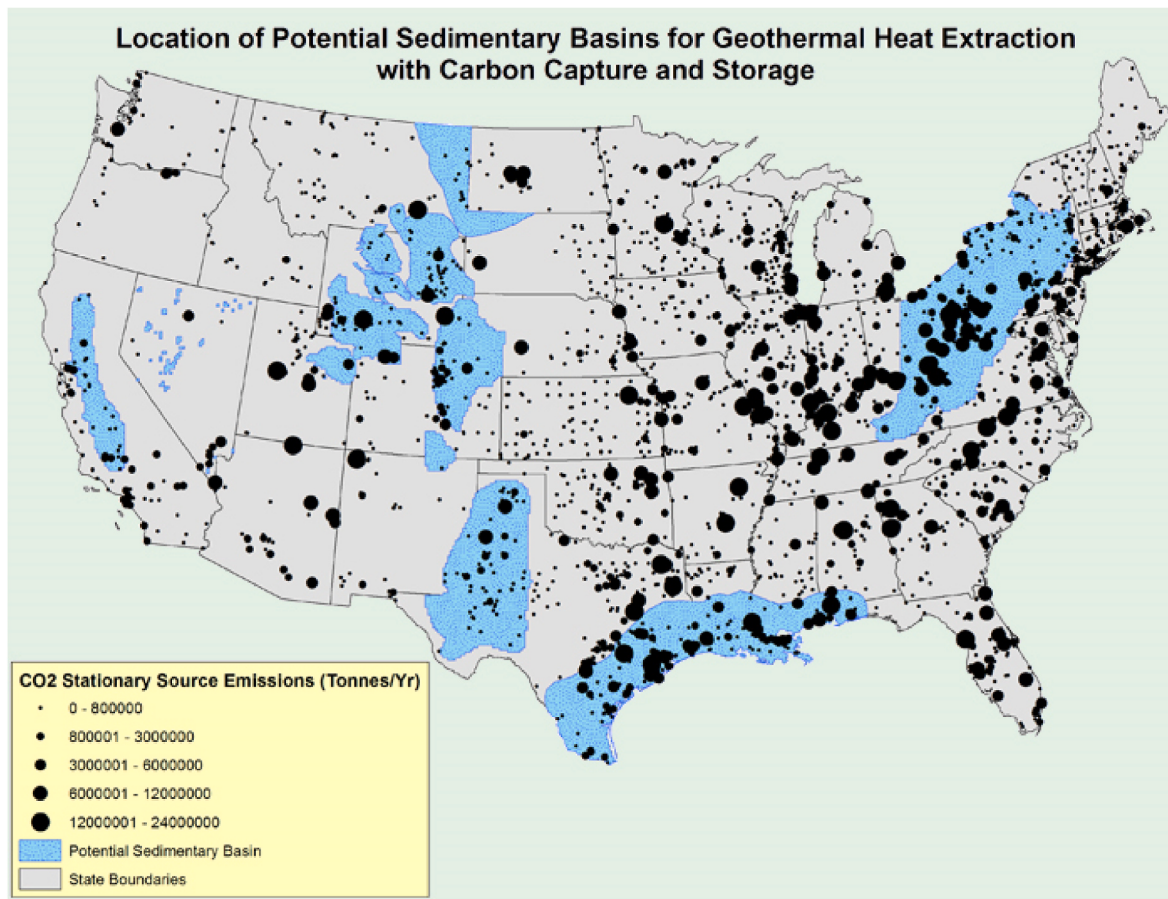


Fig. 14. Sedimentary basins in the United States superimposed on CO₂ emission sources. (Bureau of Economic Geology, 2023).

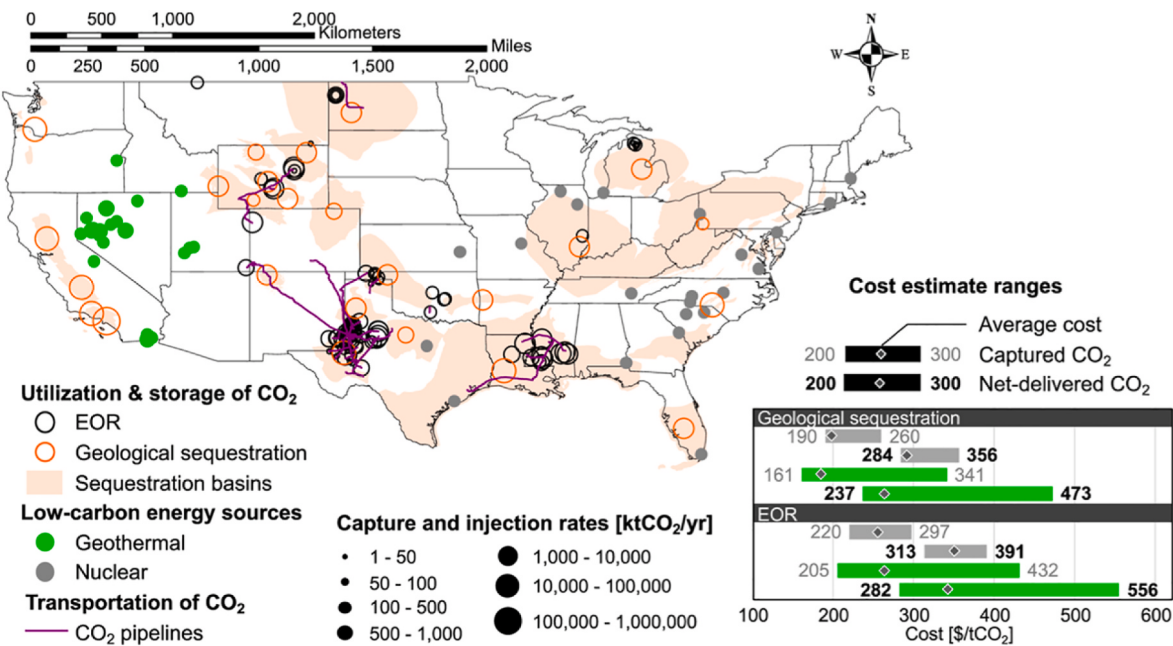


Fig. 15. Map of sequestration and EOR opportunities and geothermal and nuclear thermal resources (McQueen et al., 2020).

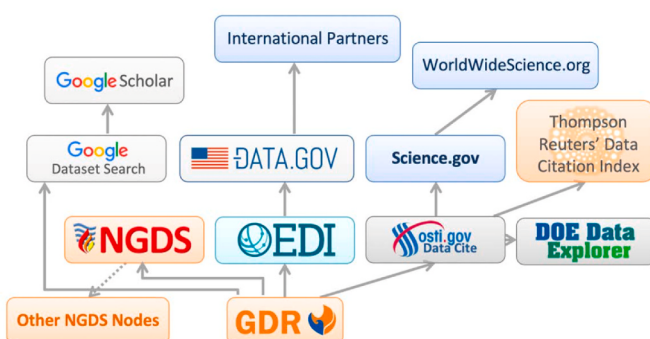


Fig. 16. Overview of GDR data sharing with a network of other databases (Weers et al., 2022).

Table 9

Top 10 countries in the world geothermal direct use and power capacity (Renewables Global Status Report, 2023 Global Status Report).

Rank	Geothermal power capacity	Geothermal direct use
1	United States	China
2	Indonesia	Turkey
3	Philippines	Iceland
4	Turkey	Japan
5	New Zealand	New Zealand
6	Mexico	Hungary
7	Kenya	Russian Federation
8	Italy	Italy
9	Iceland	United States
10	Japan	Brazil

railroad commission GISviewer can be used to view the record of oil and gas wells including BHT data. In a recent study, geothermal potential of three counties of Texas are investigated (Batir and Richards, 2022). Compared with previous studies, this work reports increase in heat flow, geothermal gradient, and thermal conductivity in the amounts of 30–40%, 13–30% and 4–20% respectively. It is worthwhile noting that temperatures of 150 °C (300 °F) have been measured in all three

counties between 3.0 and 3.5 km (9800 and 11,500 ft) depth, see Fig. 22.

A recent effort, Global Heat Flow Database (GHFD), aims to generate a geothermal gradient atlas of the world with searchable information in GIS format. As a part of this undertaking, a comprehensive publication offers a global heat flow database, see Fig. 23 (Fuchs and Norden, 2023).

A number of references in the academic literature have presented maps of geothermal gradient and heat flow for China in the past two decades. See (Wang et al., 2013), (Zhu et al., 2015) and (Wang et al., 2018) for more information. The map shown in Fig. 24 indicates the southern edge of the country has temperature suitable for S-DAC applications.

A report prepared by Geological Survey of Canada provided the temperature profiles with depth and heat flow estimations for different regions in the country (Fig. 25). Small northern communities exist in the country with high heat flow where temperatures in the range of 90–100 °C can be reached at depths as shallow as 2.5 km. This is significant for S-DAC-GT potential assessment.

Geothermal resources have been rapidly developing in Turkey in recent years. Maps of geothermal potential based on resource temperature can be found in (Basel et al., 2010) and (Ozgoren et al., 2012). It is evident that temperatures around 100 °C can be readily accessed at fairly shallow depth in Turkey, see Figs. 26 and 27.

Geothermal gradients and heat flow maps are presented by (Macgregor, 2020) for the continent of Africa based on deep well data (Fig. 28). The author reports gradients ranging from 14 °C/km in the Taoudenni Basin to over 70 °C/km in parts of the southern Red Sea.

Geothermal heat flow map of Africa (Fig. 29) in GIS format is offered by (Elbarbary et al., 2022). Surface manifestations, geological maps, faults, seismic activity map, and heat flow were investigated. Besides the obvious high geothermal potential in East Africa and countries such as Kenya and Tanzania, northern African countries such as Morocco and Libya are reported to possess geothermal gradients ranging 35–50 °C/km and 40–60 °C/km respectively.

In this section, databases and published maps suitable for geothermal prospecting were presented. It should be highlighted that temperatures around 100 °C seem accessible in various regions of the world and hence deployment of S-DAC-GT technology appears to be feasible across the planet.

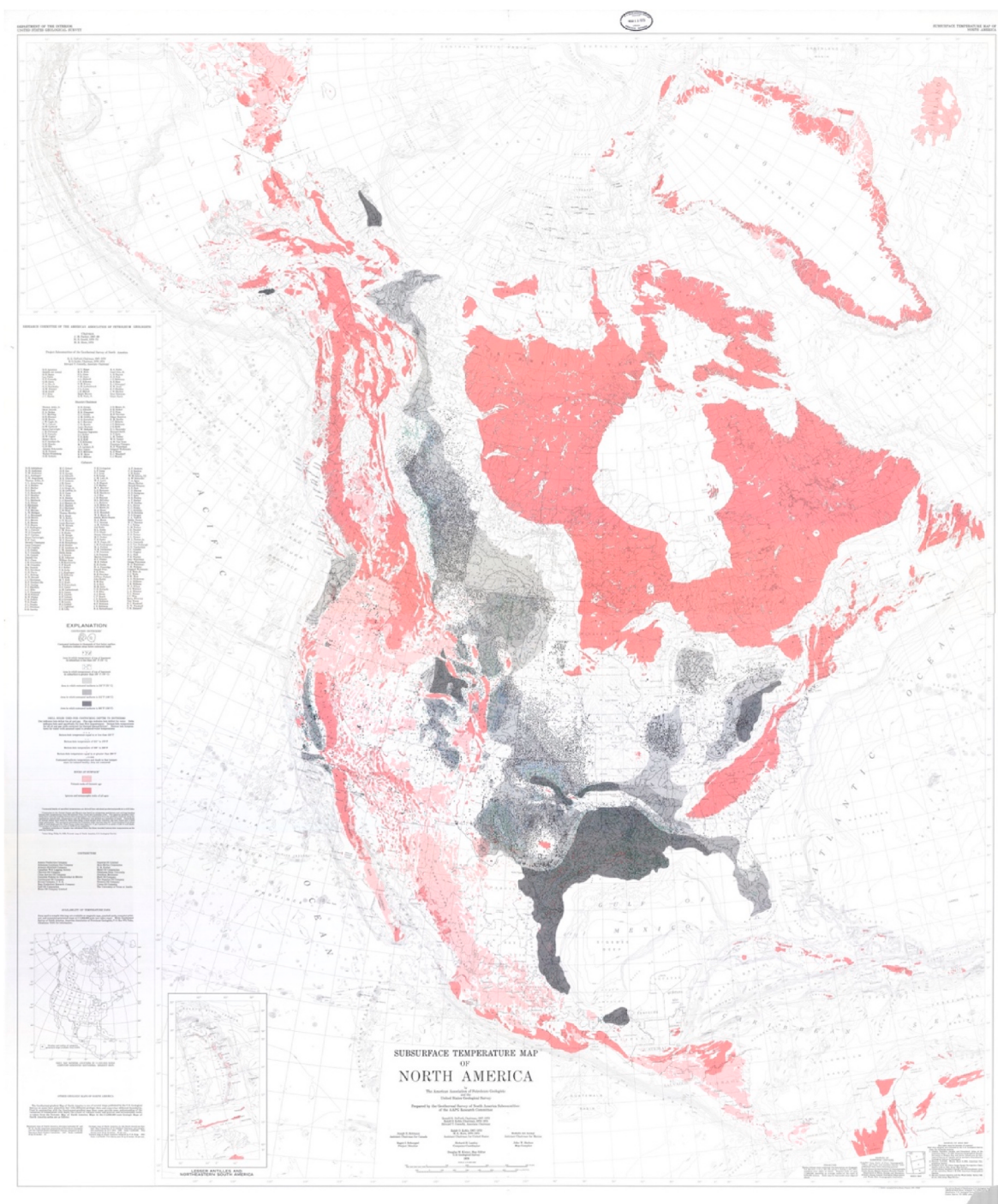


Fig. 17. Subsurface temperature map of North America - AAPG (DeFord et al., 1976).

4. Techno-economic analysis

4.1. Region selection & methodology

4.1.1. Methodology

For this analysis, we have focused on low temperature solid sorbent DAC technologies that require ~ 100 °C in order to drive the regenerative process (S-DAC). High temperature aqueous solvent technologies typically require ~ 900 °C (L-DAC). Geothermal resources at this temperature are not accessible with current technology. This analysis does not review other DAC technologies that do not require substantial thermal energy for regeneration – these other non-S-DAC and non-L-

DAC technologies require significant electrical energy; therefore, the provided electrical energy from a geothermal resource is unlikely to be substantially more efficient than electricity provided by other renewable resources.

4.1.2. Region selection

This analysis evaluates four regions as potential test cases for S-DAC powered by geothermal energy. We identified three regions within the United States, where we have deeper knowledge of geothermal resources, and there is a high regulatory and industrial appetite for large scale DAC projects. For example, Oxy Low Carbon Ventures is constructing a ~ 1 Mt/year DAC facility in West Texas using Carbon

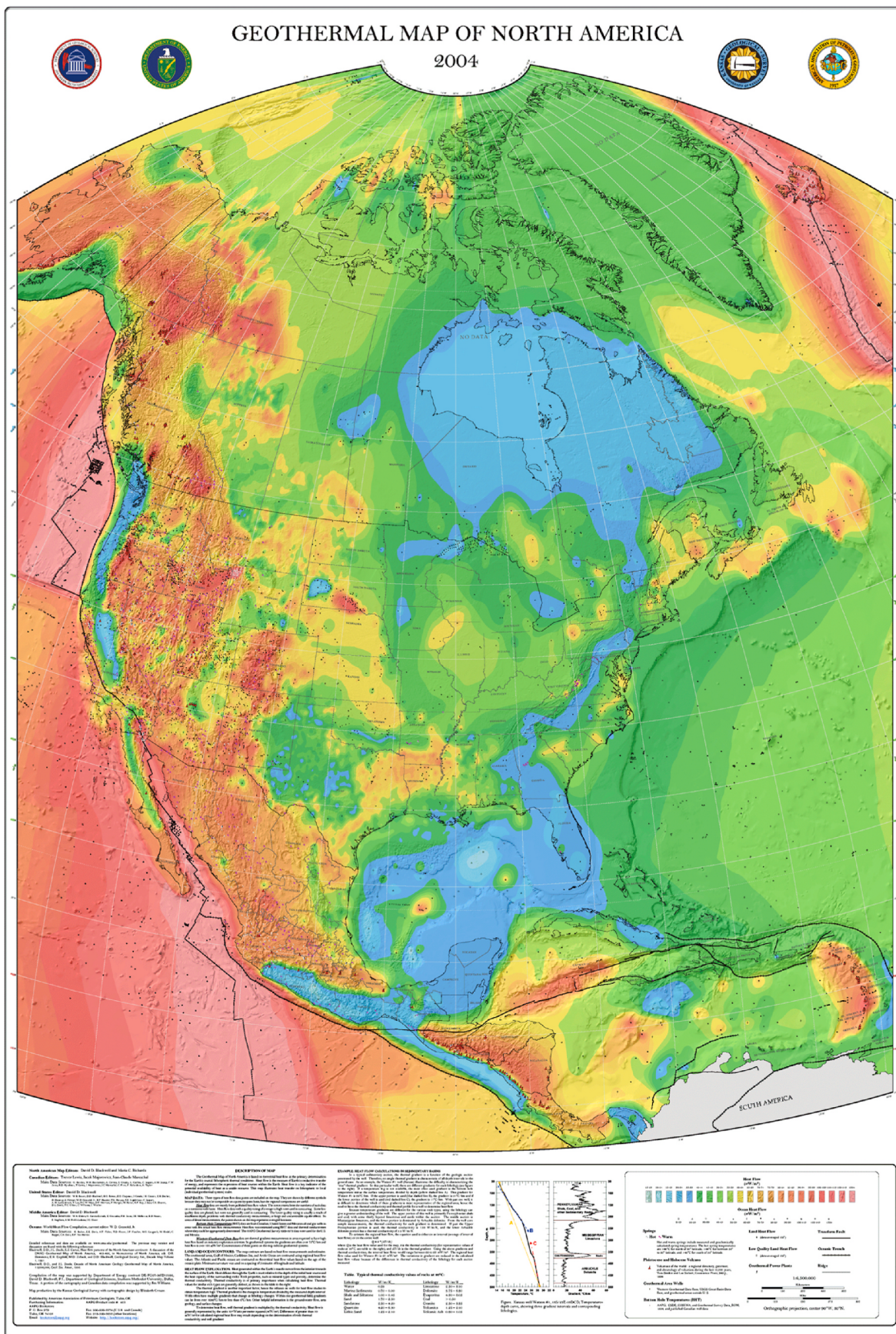
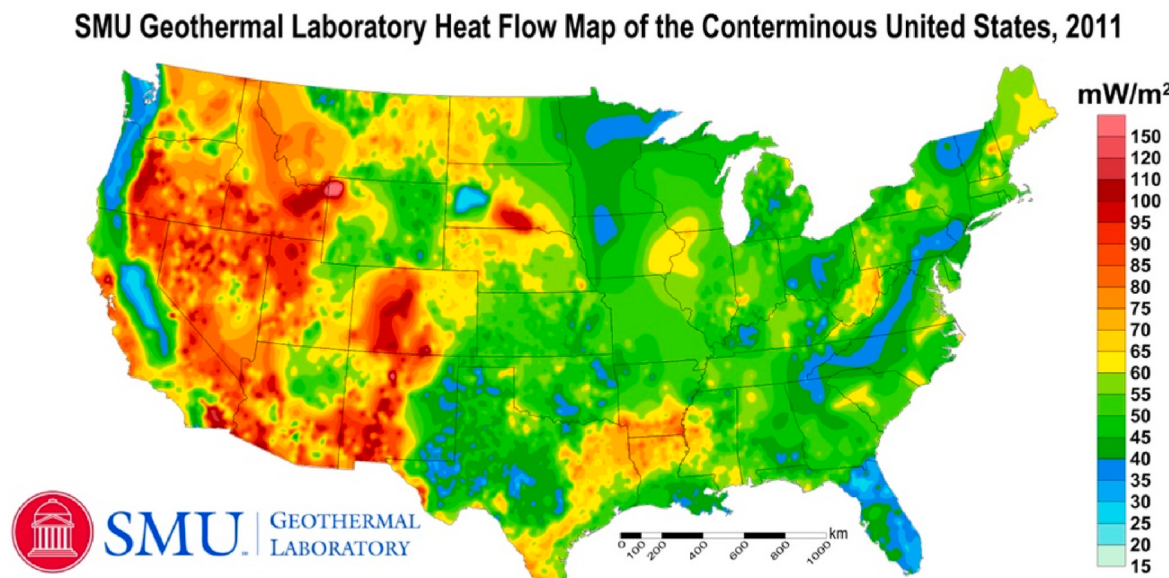


Fig. 18. Geothermal map of north America prepared by (Blackwell and Richards, 2023).



Reference: Blackwell, D.D., Richards, M.C., Frone, Z.S., Batir, J.F., Williams, M.A., Ruzo, A.A., and Dingwall, R.K., 2011, "SMU Geothermal Laboratory Heat Flow Map of the Conterminous United States, 2011". Supported by Google.org. Available at <http://www.smu.edu/geothermal>.

Fig. 19. Heat flow map of continental United States (Blackwell et al., 2011).

Engineering's aqueous solvent technology (OFX, 2022). Further, the United States passed the Inflation Reduction Act of 2022, which includes a \$180 tax credit per tonne of CO₂ geologically stored via DAC (IEA, 2022b). The revised 45Q regulations provides a further mechanism for "direct pay" rather than a tax credit (BakerHostetler, 2022), encouraging new entrant companies with innovative cost-effective DAC technologies.

We also identified one potential European basin as an alternative outside North America. The European Union has a comparatively mature CO₂ emissions trading (EU Emissions Trading System, 2022). The EU ETS CO₂ price has ranged below €100 through 2022 (EU Carbon Price Tracker), and therefore the EU market price would need to be subsidized to be comparable to United States tax credits.

To finalize the selected regions, we applied three major criteria.

1. Proven and accessible geothermal resources. These resources could be in the form of existing geothermal and hydrothermal facilities, known geothermal energy resources that can be economically accessed, or existing oil and gas wells with bottom hole temperatures near ~120 °C that could be re-purposed as high temperature brine wells with flow rates and temperatures adequate to drive the S-DAC regenerative process.
2. Regions with elevations close to sea level. Gaseous CO₂ is denser than other atmospheric gases, and ambient CO₂ concentration levels decline at higher elevations (Abshire et al., 2010).
3. Proximity to high quality sedimentary basins for CO₂ storage. The CO₂ must be permanently stored once captured. There are several alternatives to CO₂ storage, including EOR, synthetic fuels, and carbon graphene. Industry sources indicate there is little market appetite to pay for offset CO₂ emissions via DAC if the CO₂ is used for EOR applications. Also, US 45Q regulations maximize tax credits for DAC through geological storage. For this paper, we constrain the scope of permanent storage of CO₂ to injection into capped sedimentary formations rather than mineralization in mafic and ultramafic formations.

4.1.2.1. Permanent geological storage of CO₂ in sedimentary versus mafic & ultramafic formations.

We concede that mineralization of captured

CO₂ in mafic and ultramafic formations is an attractive storage solution – the permanence of sequestering CO₂ via mineralization has higher certainty than injection of CO₂ into capped sedimentary formations. An analysis of the technical merits of the permanence of mineralization versus sedimentary storage is beyond the scope of this paper. Further, mineralization at the injected volumes necessary, ~1 Mt/year, is less well understood and the economics are less proven as a potential large scale storage alternative to sedimentary storage. For example, Iceland's Orca DAC facility, using Climeworks S-DAC technology, is scaled to inject CO₂ volumes of 4 kt per year (Climeworks, 2021), not in the Mt range evaluated for this paper.

4.2. Final regions

Applying these three criteria, we have narrowed our scope and economic analysis to the following specific regions.

1. Houston area Texas Gulf Coast
2. Los Angeles Basin in California
3. Alaska's Cook Inlet
4. Netherlands Groningen Gas Field

All four of the selected target regions have the following attributes.

- They are proven and mature oil and gas producing regions. Their geologies are very well understood, and they have readily accessible capped sedimentary formations for geological storage.
- All four regions are near sea level, ensuring maximum ambient atmospheric CO₂ concentrations.
- All four have existing oil and gas wells with bottom hole temperatures in the range required for S-DAC, >100 °C.
- An added benefit is that all four regions have concentrated presence of energy technology service companies whose expertise and infrastructure would substantially accelerate any major DAC project.

For clarity, the specific sedimentary formation for storage of CO₂ and the sedimentary formation for the extraction of geothermal energy are separate. These sedimentary formations may be overlaying or adjacent, but they are expected to be geologically isolated from each other. Geological storage of CO₂ in sedimentary formations requires extremely

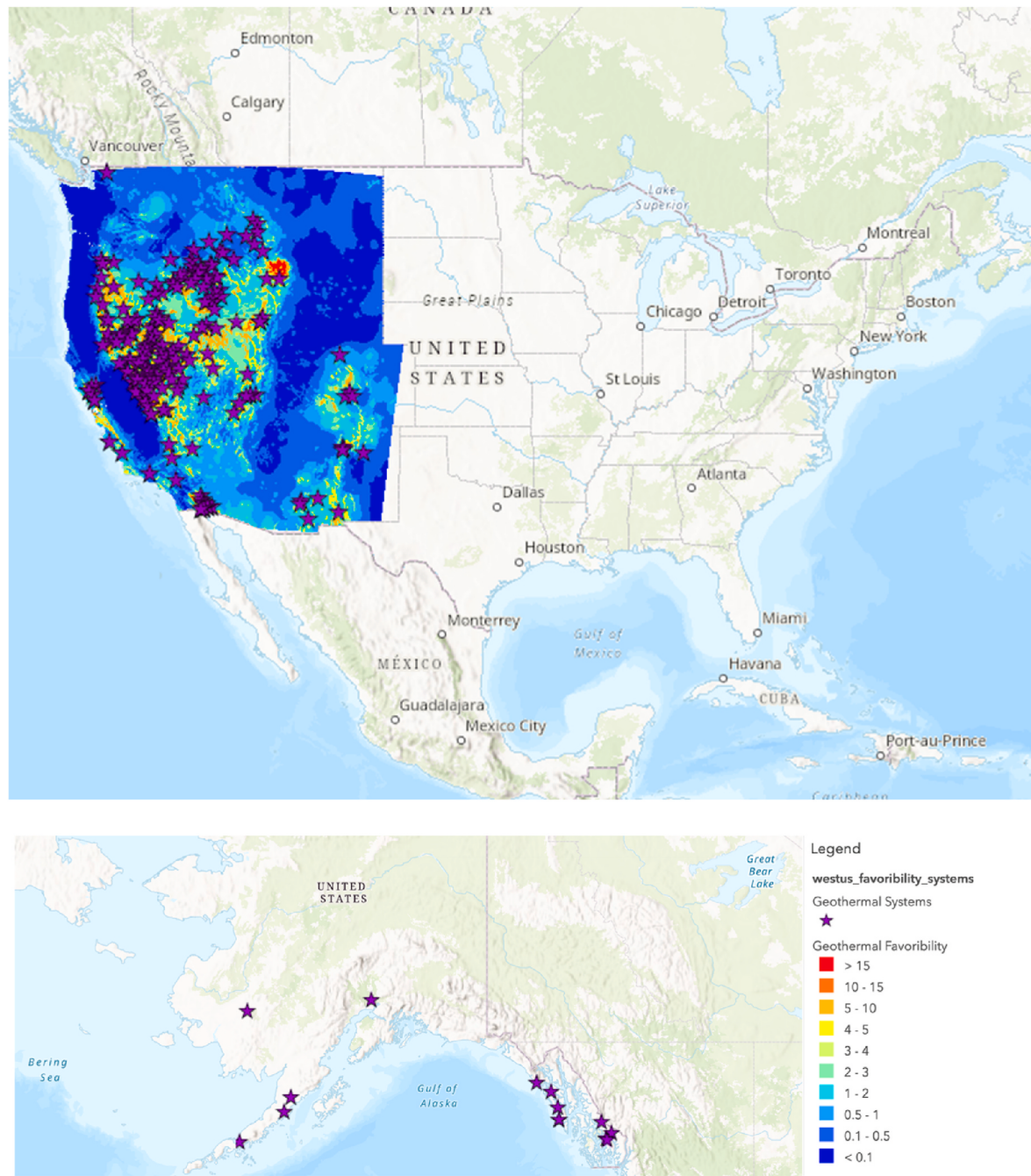


Fig. 20. Geothermal favorability map (Western United States Geothermal Favorability |U.S. Geological Survey).

high confidence of permanence. Our analysis assumes no injection of compressed CO₂ into the formation from where the geothermal brine is produced. A detailed determination of the targeted specific geological structure for CO₂ storage, or specific locations of geothermal production and injection wells, is beyond the scope of this paper.

4.2.1. Regional CO₂ storage capacity – qualitative assessment

All four regions are estimated to have extensive potential for CO₂ storage, either into depleted oil and gas fields, saline aquifers, or both.

The Texas Gulf Coast has very high-quality potential reservoirs for large scale CO₂ storage. Within Texas State waters, there is estimated approximately 30 Gt of storage capacity (Meckel et al., 2019). Depleted oil and gas wells alone in the offshore Texas Louisiana region are estimated to have CO₂ capacity of 139 Mt (Trevino, 2019).

The Los Angeles Basin is structurally complex as a potential storage

reservoir, tectonically active, with thousands of legacy wells that increase likelihood of potential leaks and complicate monitoring. A 2022 Schlumberger analysis indicated that 20 Mt of storage was feasible directly within the Basin (Cook et al., 2020). Southern California overall is estimated to have 806 Mt of CO₂ storage capacity in oil and gas fields, but this includes EOR applications (Kim et al., 2022). A more attractive storage resource may be in the southern San Joaquin basin. This basin is estimated to have storage potential of 16.6–52.0 Gt of CO₂ within its saline aquifers (Kim et al., 2022). However, accessing this basin from the Los Angeles Basin would require a CO₂ pipeline up to 200 km in length.

The Cook Inlet Basin in Alaska, though subject to regional tectonically activity, is estimated to have safe CO₂ storage capacity of between 0.91 and 16.61 Gt of CO₂ within the Hemlock formation (Pantaleone and Bhattacharya, 2020).

The Groningen gas field in northern Netherlands is estimated to have

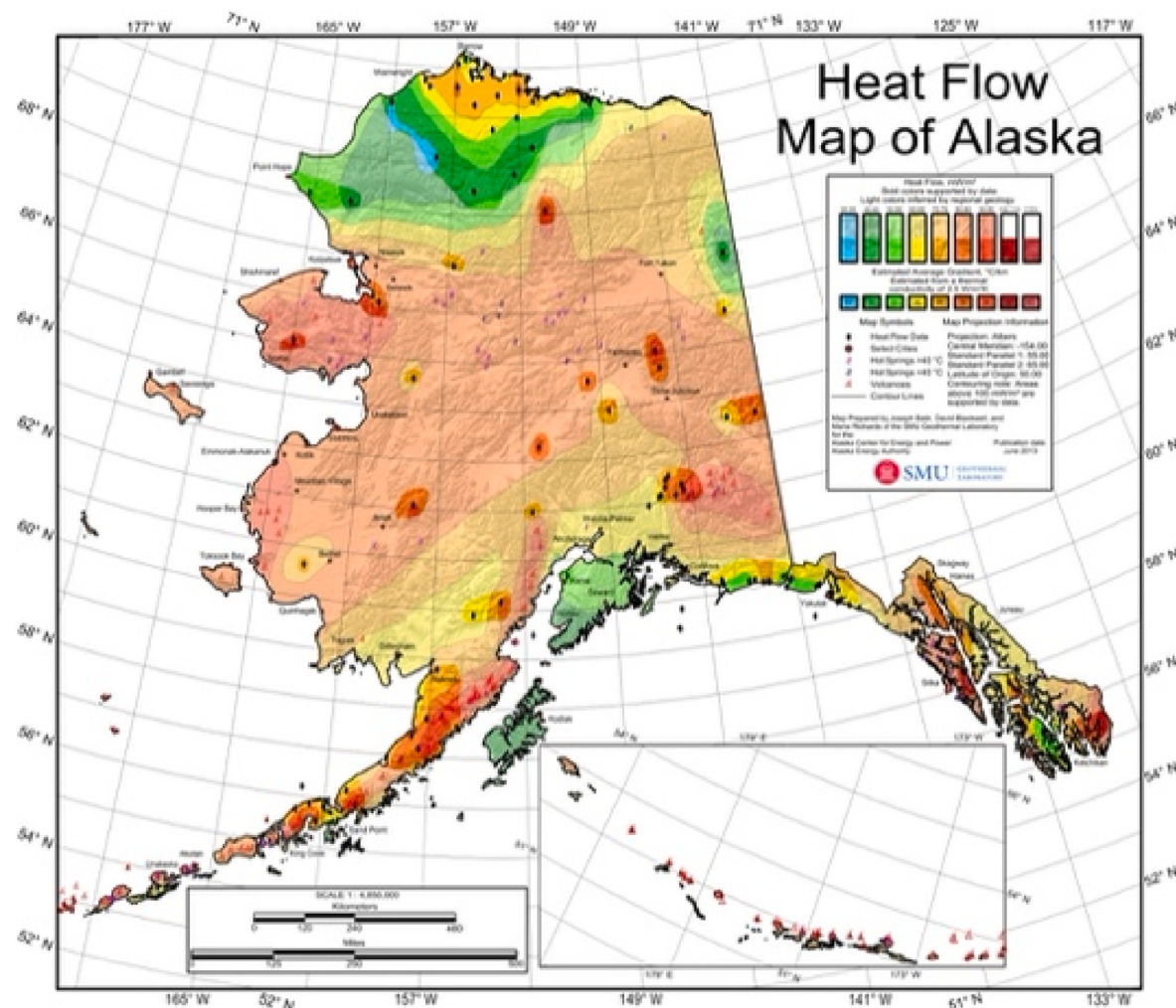


Fig. 21. Heat flow map of Alaska (Batir et al., 2013).

approximately 7.35 Gt of CO₂ storage capacity (Kay Damen and André Faaij and Wim, 2009). However, the field has been evaluated more as a potential energy storage hub for natural gas and H₂ (Juez-Larré et al., 2019) than CO₂ storage. This may be due to historic lack of public support within the Netherlands for onshore geological carbon storage, probably due to the perceived risks of CO₂ storage in conjunction with the Netherlands high population density (Akerboom et al., 2021). The Dutch government has, on the other hand, sponsored offshore CCS projects. Offshore storage in saline aquifers off the western coast of the Netherlands, with estimated storage capacity of 1.6 Gt of CO₂, may be a more politically attractive option (Siebels et al., 2022). This option would require a CO₂ pipeline up to 200 km in length.

4.3. Cost of carbon storage

There is substantial high-quality data and research estimating the costs of transportation, compression, injection, and storage monitoring of CO₂ in sedimentary formations (collectively referred to as “carbon storage”), and several ongoing projects that prove the viability of the technology. As a result, there is greater certainty around the costs of carbon storage than DAC. The National Academy of Sciences consolidated a robust study of the cost of carbon storage, and estimated a levelized cost range of \$8.6 to \$20.4 per tonne of CO₂ (National Academies of Sciences, 2019). This number is relatively small compared to the cost of capture by DAC; therefore, for this analysis, we have not pursued further precision for the cost of carbon storage.

However, it is important to note that the costs of carbon storage will be influenced by pipeline requirements and the economies of scale due to the presence of other large stationary CO₂ emitters within the region. For example, the Cook Inlet maybe less economically attractive for CO₂ storage as it has fewer regional CO₂ emitters. The Great Plains Institute identified 14 potential US CO₂ storage hubs based on the scale of stationary emissions in the region, specifically tying geological storage potential to regional sources of emissions (Abramson et al., 2023). The Great Plains list includes the greater Los Angeles region and the Houston Gulf Coast area as likely future CO₂ storage hubs, but not Alaska. The reason is that both the Los Angeles Basin and Houston Gulf Coast have combined regional point sources of CO₂ emissions greater than 30 Mt/year. In comparison, the wider Cook Inlet region, despite being adjacent to Anchorage’s industrial infrastructure, has only ~3 Mt/year of CO₂ point source emissions (NETL, 2022). With respect to the Groningen Gas Field, cumulative co-located stationary emissions in northern Netherlands is estimated as less than 10 Mt. However, the field is within ~150 km of >30 Mt/year of stationary emissions around Munster, Germany (Patricio et al., 2017). Pipeline costs to transport CO₂ from the Los Angeles Basin and the Groningen Gas Field to more attractive storage locations, as discussed in the Regional CO₂ Storage Capacity section, may be mitigated by economies of scale transporting other adjacent CO₂ emissions. Nevertheless, this carbon storage cost differential does not significantly move the needle relative to the cost of S-DAC. In this techno-economic analysis, we assume \$20/tonne CO₂ storage cost for all four regions.

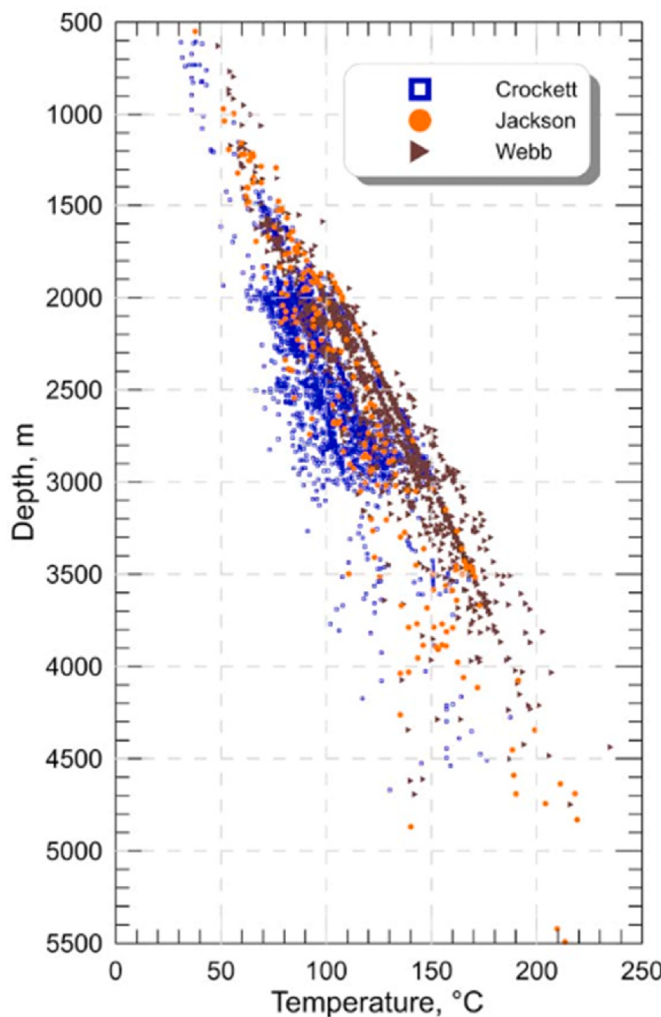


Fig. 22. Updated geothermal potential map of three Texas counties (Batir and Richards, 2022).

4.4. DAC economic model

There are many cost models for DAC, as discussed in the literature review section. This paper relies on three primary sources for S-DAC costs and energy requirements.

- Techno-economic assessment of CO₂ direct air capture plants (Fasihi et al., 2019)
- Negative Emissions Technologies and Reliable Sequestration: A Research Agenda by the National Academies of Sciences, Engineering, and Medicine (National Academies of Sciences, 2019)
- Direct Air Capture Case Studies: Sorbent System by the National Energy Technology Laboratory (Valentine et al., 2022)

There remains a wide range of cost projections with a great deal of uncertainty, as the technology is relatively new, continually improving, with potentially large efficiencies of scale. Cost estimates can range from \$100 to \$1000 per tonne CO₂. The NAS 2019 report alone provides a range of \$18 to \$1,075, although the report readily acknowledges the extremes of the ranges are unlikely (National Academies of Sciences, 2019). A summary of the model parameters is provided in Table 10.

It is not the goal of this paper to create false precision on the potential costs of DAC at scale. Rather, this techno-economic analysis has two objectives: determine a range of costs savings using geothermal resources for thermal energy and provide a relative comparison of potential costs of S-DAC and S-DAC-GT across the four regions

Each of the three cost models uses different assumptions. We have used the “mid” cost range estimated by NAS 2019. NAS 2019 assumes a 1 Mt/year facility, Fasihi et al., 2019 assumes 0.36 Mt/year, and NETL, 2023 assumes 0.1 Mt/year. We have not attempted to normalize for scale. Rather, we have normalized for inflation and currency, assuming USD at mid-2022 pricing levels, a cost of capital (WACC) of 10%, and a project lifetime of 20 years.

We have normalized CAPEX and OPEX for US regional cost variations using the following methodology. For CAPEX, we assumed pipeline construction costs are a reasonable proxy for large capital projects; these costs also reflect regulatory differences and geographical challenges. A direct comparison of pipeline costs between Alaska and Texas Gulf Coast is possible by reviewing estimated budgets for major natural gas pipeline projects: the proposed Alaska LNG pipeline (AKLNG) and the proposed onshore Rio Bravo Gas Pipeline along the Texas Gulf Coast (Oil and Gas

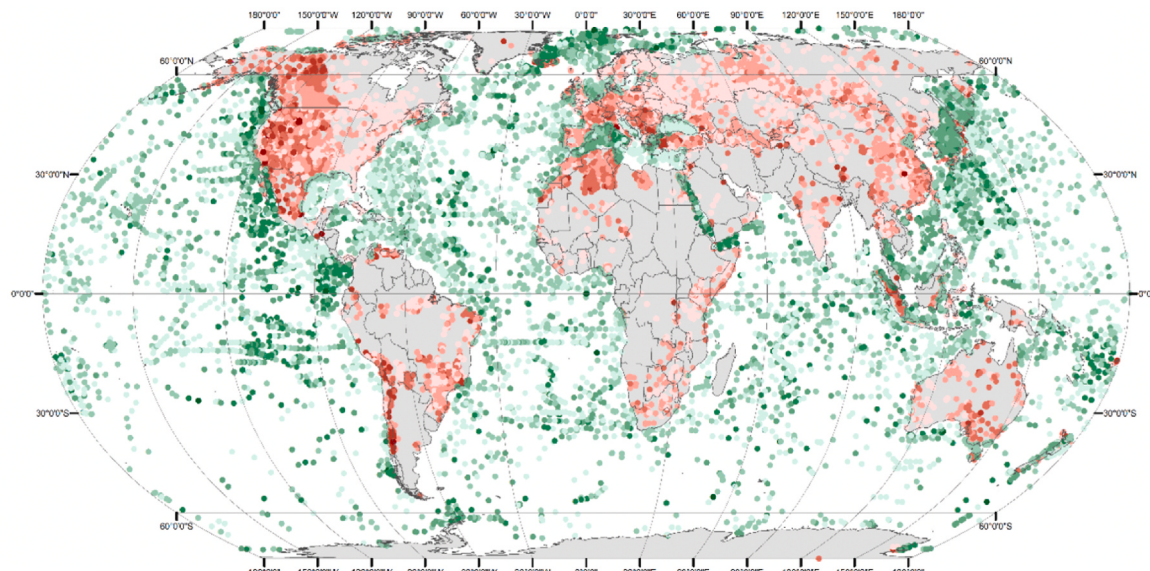


Fig. 23. Global map of heat flow (Fuchs and Norden, 2023).

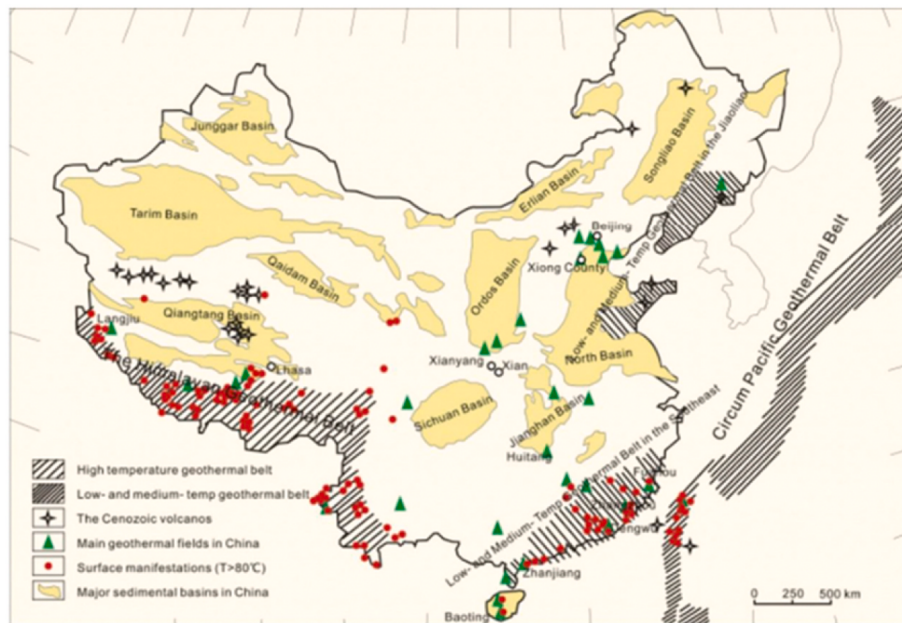


Fig. 24. Temperature map for China (Zhu et al., 2015).

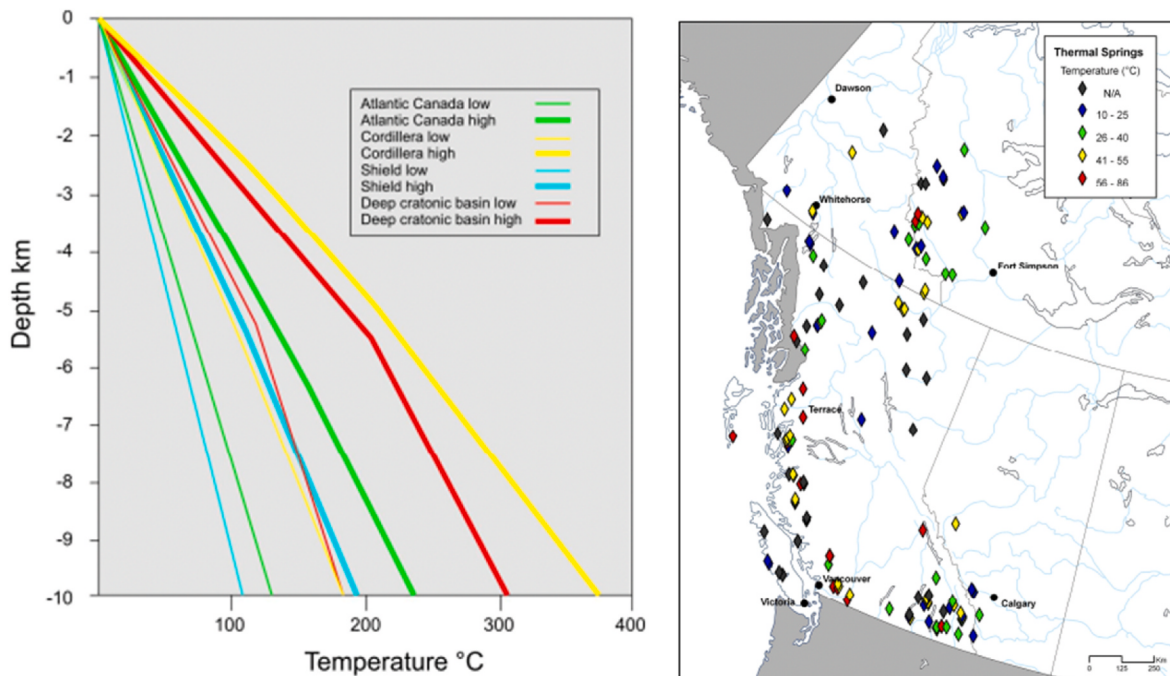


Fig. 25. Temperature profiles with depth and heat flow estimations for Canada.

(Pipeline Construction Costs, 2021). Similarly, in order to estimate CAPEX variations between California and Texas, we relied on the American Petroleum Institute's 2017 study, which provides regional cost multipliers for pipeline construction (Petak et al., 2017).

For OPEX, we used Regional Price Parities from the US Bureau of Economic Analysis, which details cost factors by state for 2020 (BEA, 2021).

We have not normalized CAPEX and OPEX costs in the Netherlands versus the US. Due to recent increases in global inflation rates, coupled with large variations in national inflation rates, there is greater volatility in national cost of living factors and purchase power parity measurements. Therefore, we have relied on the currency exchange rate and

regional energy prices to reflect potential cost differences.

Our model compares costs using thermal energy required for S-DAC from either electricity or local geothermal resources. We evaluate CO₂ emissions associated with each region's electricity production in the Carbon Footprint of DAC section below.

We used industrial electricity prices for the first half of 2022 for each region. Our sources are the US Energy Information Administration (EIA, 2022b) and the EU's Eurostat databases (Eurostat, 2023; *eurostat Data Browser*), which provide rates by state or country and by type of customer. We applied the exchange rate of 1.094 USD to EUR, the average exchange rate for the 1st half of 2022 (OFX (US) *Monthly average rates*, 2022). Regional cost factors are included in Table 11.

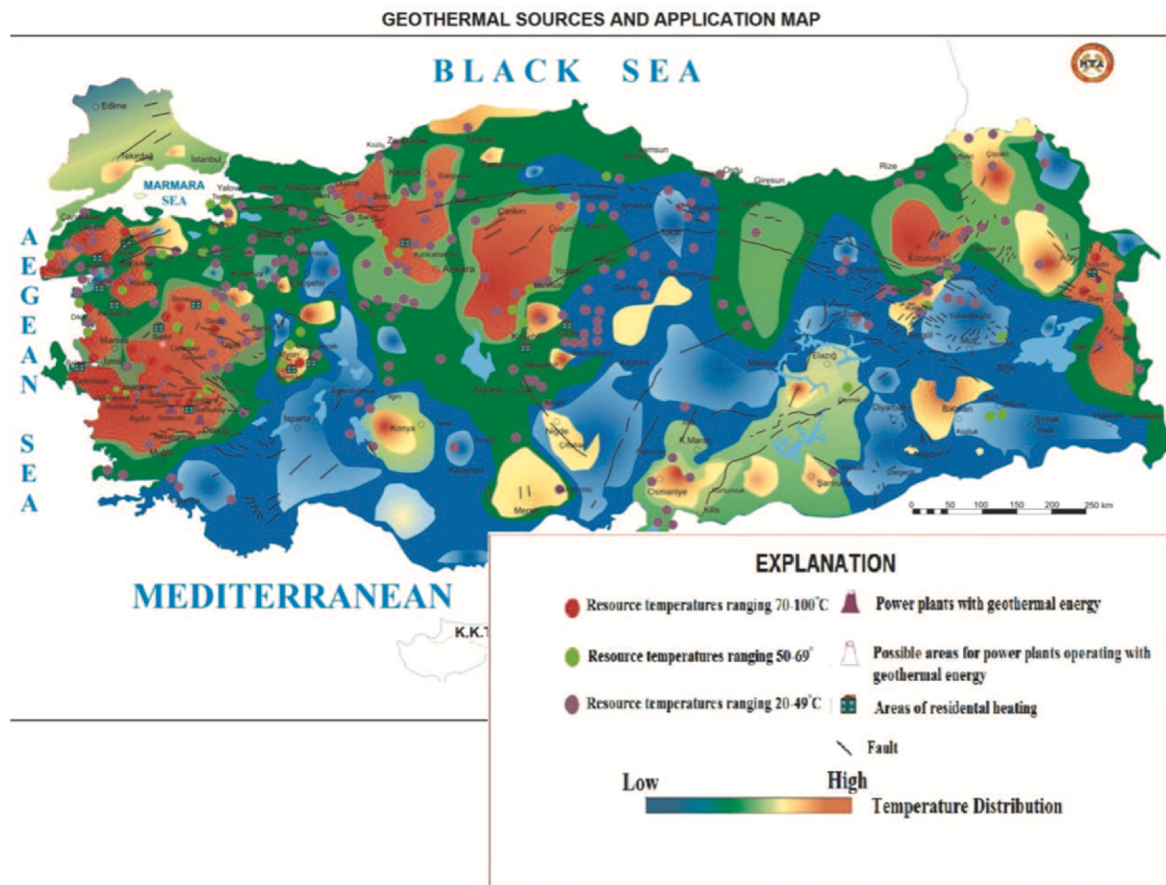


Fig. 26. Temperature profiles with depth and heat flow estimations for Turkey (Ozgoren et al., 2012).

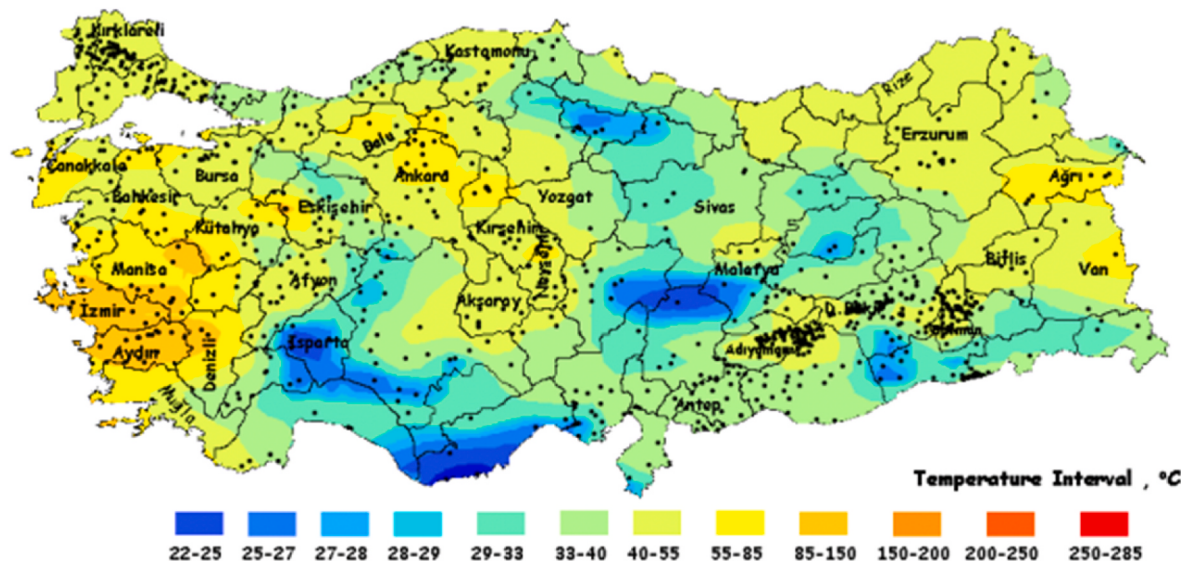


Fig. 27. 1000 m depth temperature distribution map with kriging in Turkey (Basel et al., 2010).

S-DAC efficiency can be substantially affected by humidity and temperature. We normalize the amount of thermal energy required for the S-DAC process based on the paper, *Optimal Design and Operation of Solid Sorbent Direct Air Capture Processes at Varying Ambient Conditions* (Wiegner et al., 2022) using average annual temperature and humidity in each region.

Summary of the regional cost factors, weather factor (Therm Index),

drilling depth, and electricity prices are captured in Table 11.

Geothermal thermal energy cost estimates are obtained from the National Renewable Energy Laboratory's 2016 report: *Low Temperature Geothermal Resource Assessment for Membrane Distillation Desalination in the United States* (Akar, 2016). The report provides a robust cost model of depleted oil and gas wells repurposed as sources for low temperature (90°C) thermal energy extraction.

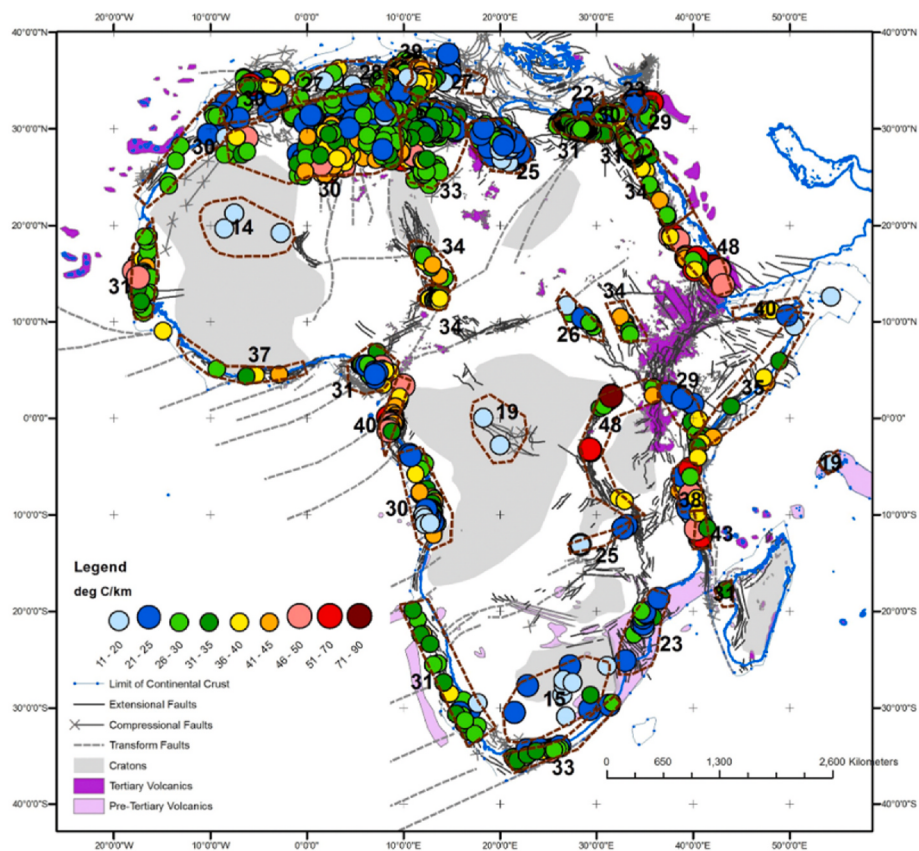


Fig. 28. Temperature profiles with depth and heat flow estimations for African Basins (Macgregor, 2020).

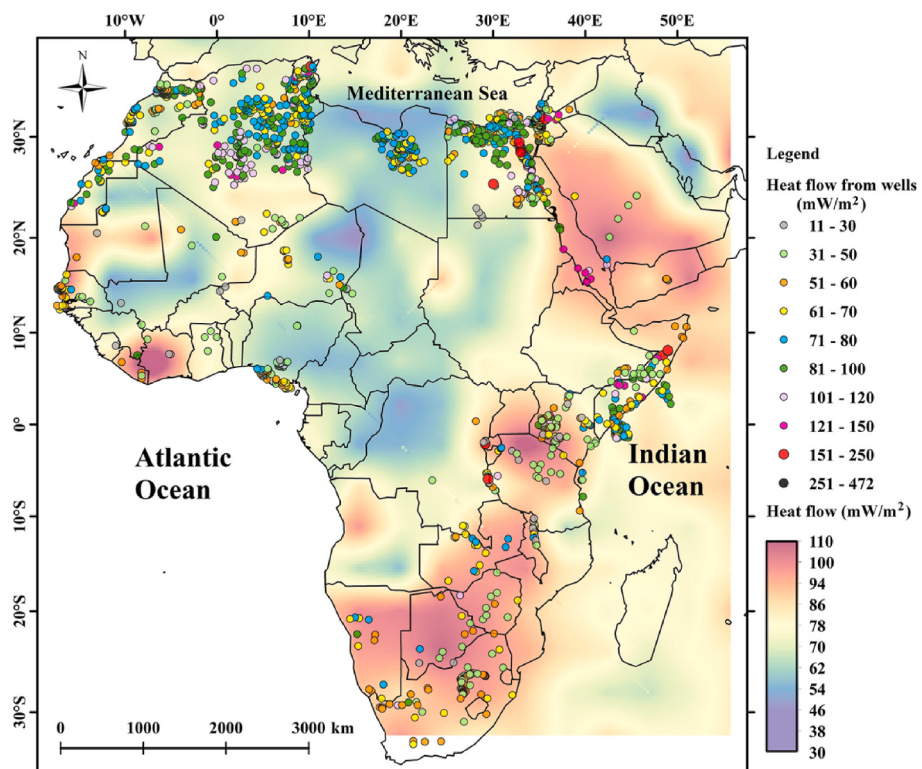


Fig. 29. Temperature profiles with depth and heat flow estimations for Africa (Elbarbary et al., 2022).

Table 10
Model parameters.

\$ per tonne CO ₂	CAPEX*	OPEX	MW _e	MW _{th}
Fasihi et al., 2019	109.83	37.40	0.25	1.75
NAS 2019	151.74	17.05	0.23	1.14
NETL, 2023	224.23	115.00	2.27	1.45

* Normalized for 10% WACC, exchange rates (if applicable) and 2022 H1 inflation.

Table 11
Regional cost factors.

	CAPEX Factor	OPEX Factor	Therm Index	Depth	Electricity
				ft	\$/kWh
Texas Gulf Coast	1.00	1.00	1.10	10,700	0.0645
Los Angeles Basin	1.27	1.11	1.10	11,300	0.1493
Alaska Cook Inlet	1.99	1.04	0.50	17,375	0.1700
Netherlands Groningen Gas Field	1.00	1.00	0.60	11,500	0.0943

Table 12
Regional geothermal energy costs.

(\$/kWh _{th})	New Well	Existing Well
Texas Gulf Coast	0.0177	0.0086
Los Angeles Basin	0.0233	0.0135
Alaska Cook Inlet	0.0353	0.0201
Netherlands Groningen Gas Field	0.0231	0.0134

Table 13
Levelized cost of DAC by region.

(\$ per tonne)	Baseline	Geothermal	Geothermal
	100% Electrical	New Well	Existing Well
Texas Gulf Coast	410	329	315
Los Angeles Basin	676	467	451
Alaska Cook Inlet	711	600	589
Netherlands Groningen Gas Field	533	410	401

S-DAC requires temperatures on the range of ~100 °C. Specifically, Climeworks' system uses a temperature swing of 120 °C–80 °C (Beutler et al., 2019). Assuming a target geothermal resource temperature of 120 °C, we use basin specific temperature gradients and bottom hole temperatures to determine the drilling depth required within each region. We take into account drilling efficiency improvements since 2016 based on the EIA's Drilling Productivity Report through September 2022 (EIA, 2022a). Further, we normalize the geothermal cost model for CAPEX and OPEX costs as we did for the S-DAC facilities. Similarly, the model is normalized for a cost of capital (WACC) of 10%, a project lifespan of 20 years, using mid-2022 price levels (BLS, 2022). The calculated regional geothermal energy costs for a new well and existing well are presented in Table 12.

Applying these assumptions and taking the averages of outputs from the three economic models, we arrive at the leveled costs of S-DAC by region in Table 13.

4.4.1. Geothermal production temperature over time

One deficiency in our model is our assumption that the extracted geothermal brine remains 120 °C. This is unlikely to remain the case through the lifetime of the project, as thermal drawdown has been observed in every geothermal energy play. Well design and reservoir

Table 14
Regional electricity carbon intensity and cost.

	CO ₂ emissions tonne/MW _e	Electricity cost \$/kWh _e
Texas Gulf Coast	0.428	0.065
Los Angeles Basin	0.229	0.149
Alaska Cook Inlet	0.539	0.170
Netherlands Groningen Gas Field	0.418	0.094

Table 15
CO₂ emissions per unit captured via DAC.

CO ₂ emitted/DAC	Baseline	Natural Gas	Geothermal
	(100% electric)	(thermal energy only)	(thermal energy only)
Texas Gulf Coast	1.073	0.703	0.422
Los Angeles Basin	0.573	0.520	0.226
Alaska Cook Inlet	0.884	0.635	0.522
Netherlands Groningen Gas Field	0.746	0.552	0.400

engineering decisions can play a large role in mitigating this drawdown. Given our assumed re-injection temperature is 80 °C, if we assume a decline in produced temperature to 100 °C, the effective average decline in savings relative to Baseline DAC cost can range from 2.0 to 6.9 percentage points, average 3.8 percentage points.

4.5. Carbon Intensity of DAC

As DAC is an energy intensive process, it is important to assess the CO₂ emissions, or "carbon intensity", of the process to determine the net CO₂ captured. Each region's electricity carbon intensity is determined by the fuel profile of its power industry. Higher electricity prices observed in California may be correlated to the low carbon intensity of its electricity infrastructure. Regional electricity profiles are presented in Table 14.

We evaluated the carbon intensity of the DAC within each region comparing three alternative processes.

- 1) Thermal energy generation using 100% electricity, with its regional carbon intensity profile
- 2) Thermal energy generation using natural gas, for comparison
- 3) Thermal energy generation using regional geothermal resources

As a reminder, in our model, we assume geothermal resources are used exclusively for thermal energy production. Therefore, the geothermal energy facility requires electricity from the regional grid, and it cannot be assumed to be carbon neutral. The regional carbon intensity of the geothermal resource will depend on the regional electricity carbon intensity profile. Our model assumes no difference in total electricity consumed for a new or existing geothermal well – the primary use of electricity is the injection and extraction of the high temperature brine, which is predominantly a function of the depth of the geothermal reservoir.

As regional electricity supplies become more reliant on renewable sources, the CO₂ emissions associated with DAC will decline and the carbon intensity will improve. In an ideal future where the electricity supply is fully generated by renewable sources such as wind, solar, and geothermal, and other zero-emissions sources such as hydro and nuclear, the carbon intensity of DAC would improve to zero.

Table 15 summarizes the carbon intensity analysis.

5. Potential future studies

The available scope for future studies regarding S-DAC-GT is vast. A

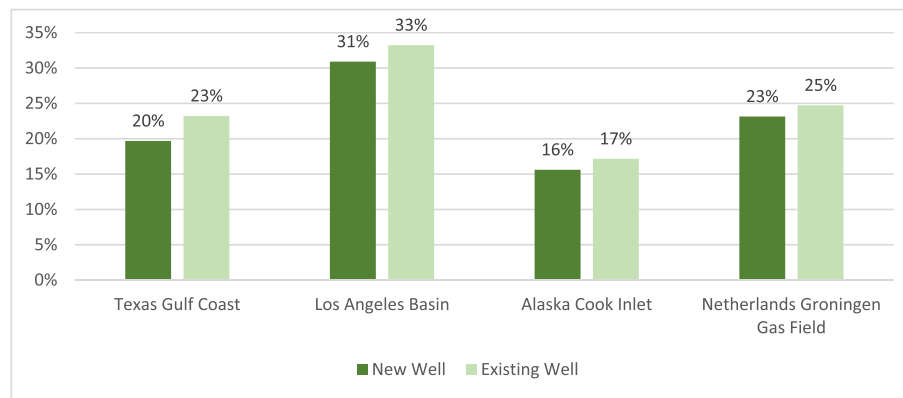


Fig. 30. Savings due to geothermal relative to baseline.

subset of potential follow-on analyses to this paper are.

- 1) **Techno-economic review of S-DAC-GT permanent geologic storage in mafic and ultramafic formations.** As explained above, this paper intentionally focuses on using sedimentary basins for CO₂ geologic storage. This is because costs and capacities of CO₂ storage through mineralization remain theoretical at volumes of ~1 MT/year. However, mafic and ultramafic formations have the benefit of being closer to higher thermal gradients and, therefore, access to shallower, hotter, and potentially cheaper geothermal reservoirs.
- 2) **Reservoir specific geothermal modeling.** This paper concedes that thermal drawdown of the geothermal reservoir is a deficiency in the analysis. This problem is highly dependent on well design, reservoir engineering, and formation characteristics. Better modeling of thermal drawdown in sedimentary reservoirs would be very useful in evaluating region specific S-DAC-GT costs.
- 3) **Reservoir specific characterization.** This paper assumes that the geothermal reservoir and the CO₂ storage reservoir are separate and isolated from each other. Further study of potential regional reservoirs would be useful in evaluating availability of CO₂ storage with adequate caprock seals, ensuring separation from the geothermal reservoir.

6. Conclusions

Our paper analyzes four primary questions associated with using geothermal resources as the source for thermal energy required in S-DAC processes.

- 1) Does use of geothermal resources reduce S-DAC costs?
- 2) How do those costs vary among the four selected regions?
- 3) How do geological storage resources compare among the four regions?
- 4) What is the carbon intensity of the S-DAC-GT process within the four regions?

6.1. Cost impact of geothermal resources on S-DAC

Our analysis concludes that geothermal energy would materially reduce the cost of S-DAC in all four regions. The savings range from 16 to 33%, depending on new vs existing geothermal wells and the region (Fig. 30). Average savings for an existing well (25%) are higher than for a new well (22%); however, it is likely some new wells would be required to meet the thermal requirements of a 1 Mt/year S-DAC facility. The highest savings were seen in the Los Angeles Basin, due to the relatively high cost of electricity in California and the relative lower cost of the available geothermal resources. The savings were comparably low

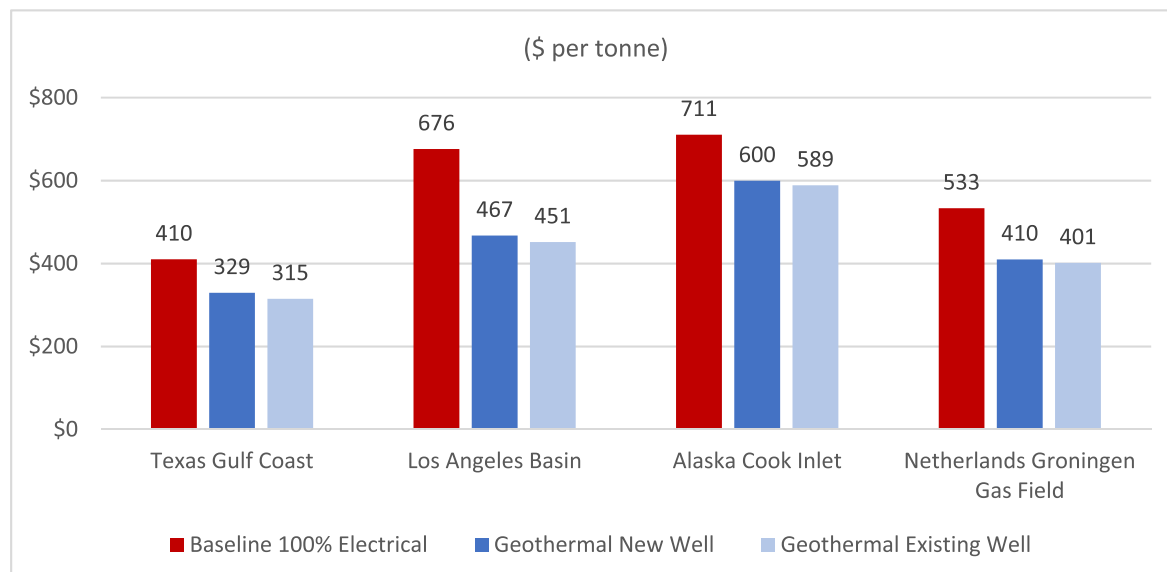


Fig. 31. Levelized cost of S-DAC.

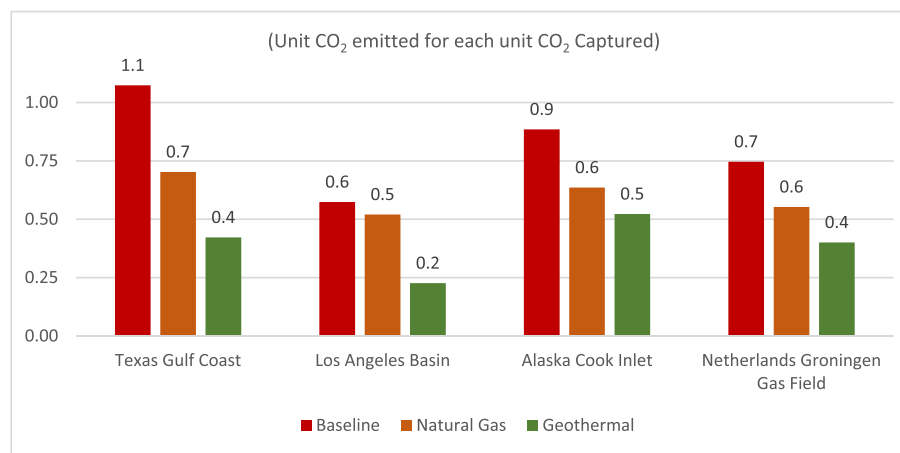


Fig. 32. Carbon efficiency of S-DAC.

for Alaska, as higher anticipated capital costs make the savings from lower cost thermal energy less relevant.

6.2. Cost variance between regions

The Texas Gulf Coast showed the lowest cost (Fig. 31). This was primarily due to having the lowest costs of electricity among all four regions and the anticipated lower cost of capital expenditures. This estimated cost disparity is consistent with the relatively lighter regulatory requirements on industries operating in Texas.

6.3. Geological carbon storage availability

All four regions have nearby geological structures for available CO₂ storage. However, additional pipelines may be required for the Los Angeles Basin and the Groningen Gas Field facilities due to potential local geological complexities (Los Angeles Basin) or political considerations (Netherlands). Alaska's Cook Inlet costs may be higher due to less economies of scale resulting from fewer regional CO₂ emitters. The Texas Gulf Coast has the most attractive storage potential with readily accessible storage geology, coupled with the likely presence of a future CO₂ storage hub supporting large regional CO₂ stationary emitters.

6.4. Carbon Intensity of S-DAC-GT

Our calculations show that without a low carbon intensity regional electricity profile, S-DAC is a very inefficient method of mitigating CO₂ emissions (Fig. 32). Even within California, with the lowest carbon intensity of the four regions analyzed, a fully electrical S-DAC system would emit 0.6 tonnes of CO₂ for each tonne captured. In Texas, due to the high carbon intensity of the grid, a 100% electric process would produce more CO₂ than it would capture. As a comparable, using natural gas to provide the thermal energy would moderately reduce the carbon intensity, but such a process in all four regions would produce at least ½ tonne of CO₂ for each tonne captured. Using geothermal resources lowers the carbon intensity to 0.4 tonnes CO₂ produced for each tonne captured in both the Texas Gulf Coast and the Netherlands Groningen Gas Field. Of the four regions evaluated, only in the Los Angeles Basin would S-DAC-GT have a capture efficiency approaching 80%.

In conclusion, S-DAC is not practical as a carbon capture process unless coupled with low carbon intensive electricity resources. Geothermal resources materially lower the carbon intensity of S-DAC in all regions. A S-DAC-GT facility in the Texas Gulf Coast would have the lowest costs, but a S-DAC-GT facility in the Los Angeles Basin would have the highest capture efficiency.

Credit author statement

Timur Kuru – Conceptualization; Data curation; Formal analysis; Investigation; Methodology; Project administration; Validation; Visualization; Roles/Writing – original draft; Writing – review & editing, Keivan Khaleghi – Conceptualization; Data curation; Formal analysis; Investigation; Methodology; Project administration; Resources; Validation; Visualization; Roles/Writing – original draft; Writing – review & editing, Silviu Livescu – Conceptualization; Data curation; Formal analysis; Investigation; Methodology; Project administration; Supervision; Validation; Visualization; Roles/Writing – original draft; Writing – review & editing.

Declaration of competing interest

The authors declare that they have no known competing financial interests or personal relationships that could have appeared to influence the work reported in this paper.

Data availability

No data was used for the research described in the article.

Acknowledgements

The authors would like to express our sincerest gratitude to Marc von Keitz, Director of The Grantham Foundation for the Protection of the Environment, and Jamie Beard, Founder and Executive Director of Project InnerSpace, for their ideas and support. Additionally, we are deeply grateful to the editors and reviewers of Geoenergy Science and Engineering, for their invaluable guidance and feedback throughout the process of writing this paper.

References

- Abramson, E., Thomiley, E., McFarlane, D., 2023. (2022). An atlas of carbon and hydrogen for United States decarbonization. Retrieved on. https://scripts.betterenergy.org/CarbonCaptureReady/GPI_Carbon_and_Hydrogen_Hubs_Atlas.pdf.
- Abshire, J., Riris, H., Allan, G., Weaver, C., Mao, J., Sun, X., Biraud, S., 2010. Pulsed airborne lidar measurements of atmospheric CO₂ column absorption. Tellus B 62, 770–783. <https://doi.org/10.1111/j.1600-0889.2010.00502.x>.
- Akar, S.A.T.C., 2016. Low temperature geothermal resource assessment for Membrane distillation desalination in the United States. Retrieved on Februray 5, 203 from. <https://www.nrel.gov/docs/fy17osti/66657.pdf>
- Akerboom, S., Waldmann, S., Mukherjee, A., Agaton, C., Sanders, M., Kramer, G.J., 2021. Different this time? The prospects of CCS in The Netherlands in the 2020s. Front. Energy Res. 9 <https://doi.org/10.3389/fenrg.2021.644796>.
- Augustine, C., Falkenstern, D., 2013. An estimate of the near-term electricity-generation potential of coproduced water from active oil and gas wells. SPE J. 19 (3), 530–541. <https://doi.org/10.2118/163142-PA>.

- BakerHostetler (2022), 2022. Inflation reduction Act provides boost and benefits to carbon capture utilization and storage industry. Retrieved. <https://www.bakerlaw.com/alerts/inflation-reduction-act-provides-boost-benefits-carbon-capture-utilization-on-storage-industry>. from.
- Basel, E.D.K., Serpen, U., Satman, A., 2010. In: Turkey's geothermal energy potential: updated results. Proceedings, 35th Workshop on Geothermal Reservoir Engineering. Stanford University, Stanford, California, pp. 1–3. <https://geo.stanford.edu/ERE/pdf/IGAstandard/SGW/2010/korkmaz.pdf>. SGP-TR-188.
- Batir, J., Richards, M., 2022. Determining geothermal resources in three Texas counties. Texas Water Journal 13 (1), 27–44. <https://twj-ojs.tdl.td.org/twj/article/view/7130/6496>.
- Batir, J.F., Blackwell, D.D., Richards, M.C., 2016. Heat flow and temperature-depth curves throughout Alaska: finding regions for future geothermal exploration. *J. Geophys. Eng.* 13 (3), 366–378. <https://doi.org/10.1088/1742-2132/13/3/366>.
- Batir, J.F., Blackwell, D.D., Richards, M.C., 2013. Updated surface heat flow map of Alaska. Retrieved on February 5, 2023 from. https://acep.uaf.edu/media/57321/HFMKA_final-report.pdf.
- BEA., 2021. Real personal consumption expenditures and personal income by state, 2020 | U.S. Bureau of Economic Analysis (BEA). Retrieved on November 1, 2022 from: <https://www.bea.gov/news/2021/real-personal-consumption-expenditures-and-personal-income-state-2020>.
- Beutler, C., Charles, L., Wurzbacher, J., 2019. The role of direct air capture in mitigation of anthropogenic greenhouse gas emissions. *Frontiers in Climate* 1. <https://doi.org/10.3389/fclim.2019.00010>.
- Blackwell, D.D., Richards, M., 2023. (2004). Geothermal map of North America: American association of Petroleum Geologists. Retrieved on from. https://www.smu.edu/~media/Site/Dedman/Academics/Programs/Geothermal-Lab/Graphics/Geothermal_MapNA_7x10in.gif?la=en.
- Blackwell, D., Richards, M., Frone, Z., Batir, J., Ruzo, A., Dingwall, R., Williams, M., 2011. Temperature-at-depth maps for the conterminous US and geothermal resource estimates. *GRC Transactions* 35. <http://pubs.geothermal-library.org/lib/grc/1029452.pdf>.
- BLS., 2022. Bureau of labor statistics data. Retrieved on, 2022. https://data.bls.gov/time-series/CUURO000SA0L1E?output_view=pct_12mths. from.
- Bonté, D., Wees, Van, J. D., Verweij, J.M., 2012. Subsurface temperature of the onshore Netherlands: new temperature dataset and modelling. *Neth. J. Geosci.* 91 (4), 491–515. <https://publications.tno.nl/publication/34612128/EH4QWt/bonte-2012-subsurface.pdf>.
- Bureau of Economic Geology, 2023. GRIDS: current research. Retrieved on. November 1, 2022 from. <https://www.beg.utexas.edu/research/programs/geothermal-research-in-deep-sedimentary-basins/current-research>.
- Climeworks, 2021. Climeworks begins operations of Orca, the world's largest direct air capture and CO₂ storage plant. Retrieved on. February 5, 2023. <https://climeworks.com/news/climeworks-launches-orca>. from.
- Cook, S., Batbayar, K., Printz, Z., 2020. Carbon Storage Potential in the Los Angeles Basin 2020 (1), 1–5. <https://doi.org/10.3997/2214-4609.202021024>.
- DeFord, R.K., Kehle, R.O., Connolly, E.T., Robinson, J.E., Schoeppel, R.J., Horn, M.K., Shelton, J.W., 1976. Subsurface temperature map of North. America. US Geological Survey. <https://doi.org/10.3133/70211242>. <https://ngmdb.usgs.gov/ProdDesc/66067.htm>.
- Deutz, S., Bardow, A., 2021. Life-cycle assessment of an industrial direct air capture process based on temperature–vacuum swing adsorption. *Nat. Energy* 6 (2), 203–213. <https://doi.org/10.1038/s41560-020-00771-9>.
- EIA, 2022a. Drilling productivity report - U.S. Energy Information Administration. Retrieved on November 1, 2022 from. <https://www.eia.gov/petroleum/drilling/>.
- EIA, 2022b. Electricity data browser. Retrieved on. <https://www.eia.gov/electricity/data/browser/>. November 1, 2022 from.
- Elbarbary, S., Abdel Zaher, M., Saibi, H., Fowler, A.-R., Saibi, K., 2022. Geothermal renewable energy prospects of the African continent using GIS. *Geothermal Energy*, 10(1) 8. <https://doi.org/10.1186/s40517-022-00219-1>.
- Fasihi, M., Efimova, O., Breyer, C., 2019. Techno-economic assessment of CO₂ direct air capture plants. *J. Clean. Prod.* 224, 957–980. <https://doi.org/10.1016/j.jclepro.2019.03.086>.
- Geothermal Technologies, O., 2019. GeoVision: harnessing the heat beneath our feet. place = United States. <https://doi.org/10.2127/1879171>.
- Glassley, W.E., Brown, E., Asquith, A., Lance, T., Perez, G., 2013. Geothermal energy potential from oil fields in the Los Angeles Basin and Co-located renewable resources. *GRC Transactions* 37. <https://publications.mygeoenerynow.org/grc/1030648.pdf>.
- IEA, 2022a. Direct air capture 2022. Retrieved on. February 5, 2023 from. <https://www.iea.org/reports/direct-air-capture-2022>.
- IEA, 2022b. Section 45Q credit for carbon oxide sequestration. Retrieved on, 4 November, 2022 from. <https://www.iea.org/policies/4986-section-45q-credit-for-carbon-oxide-sequestration>.
- Juez-Larré, J., van Gessel, S., Dalman, R., Remmelts, G., Groenenberg, R., 2019. Assessment of underground energy storage potential to support the energy transition in The Netherlands. *First Break* 37 (7), 57–66. <https://doi.org/10.3997/1365-2397.n0039>.
- Kim, T.W., Callas, C., Saltzer, S.D., Kovsek, A.R., 2022a. Assessment of oil and gas fields in California as potential CO₂ storage sites. *Int. J. Greenh. Gas Control* 114 (103579). <https://doi.org/10.1016/j.ijggc.2022.103579>.
- Kim, T.W., Yaw, S., Kovsek, A.R., 2022b. Evaluation of geological carbon storage opportunities in California and a deep look in the vicinity of kern county. In: SPE Western Regional Meeting. California, Bakersfield. <https://doi.org/10.2118/209340-MS>. USA, April. SPE-209340-MS.
- Macgregor, D.S., 2020. Regional variations in geothermal gradient and heat flow across the African plate. *J. Afr. Earth Sci.* 171 <https://doi.org/10.1016/j.jafrearsci.2020.103950>.
- McQueen, N., Psarras, P., Pilorgé, H., Liguori, S., He, J., Yuan, M., Wilcox, J., 2020. Cost analysis of direct air capture and sequestration coupled to low-carbon thermal energy in the United States. *Environ. Sci. Technol.* 54 (12), 7542–7551. <https://doi.org/10.1021/acs.est.0c00476>.
- Meckel, T.A., Hovorka, S., Trevino, R., 2019. What offshore CCS will look like in the Gulf of Mexico - perspectives from Texas. In: Offshore Technology Conference. Texas, Houston. <https://doi.org/10.4043/29268-MS>. May. OTC-29268-MS.
- Mordensky, S.P., Lipor, J.J., Deangelo, J., Burns, E.R., Lindsey, C.R., 2022. Predicting geothermal favorability in the western United States by using machine learning. In: Addressing Challenges and Developing Solutions. Proceedings, 47th Workshop on Geothermal Reservoir Engineering. Stanford University, Stanford, California. <https://pangea.stanford.edu/ERE/db/GeoConf/papers/SGW/2022/Mordensky.pdf>. February 7–9. SGP-TR-223.
- National Academies of Sciences, E., and Medicine, 2019. Negative Emissions Technologies and Reliable Sequestration: A Research Agenda. The National Academies Press. <https://doi.org/10.17226/25259>.
- NETL, 2022. CO₂ stationary sources. Retrieved on. <https://www.netl.doe.gov/node/6096>. February 5, 2023 from.
- OFX, 2022. Monthly average rates. Retrieved on. <https://www.ofx.com/en-us/forex-news/historical-exchange-rates/monthly-average-rates/>. November 1, 2022 from.
- Oil and gas pipeline construction costs, 2021. Retrieved on. https://www.gem.wiki/Oil_and_Gas_Pipeline_Construction_Costs. November 1, 2022 from.
- Ozgoren, M., Kocak, S., Canli, E., Aksoy, M.H., Dogan, S., 2012. Developments, applications and policies of renewable energy in Turkey. *Energy* 6, 8QLYHUVLW, 7XUNH.
- Pantaleone, S., Bhattacharya, S., 2020. Potential for carbon sequestration in the Hemlock formation of the cook Inlet Basin, Alaska. *Environ. Geosci.* 27 (3), 143–164. <https://doi.org/10.1306/eg.10221919011>.
- Patrício, J., Angelis-Dimakis, A., Castillo-Castillo, A., Kalmykova, Y., Rosado, L., 2017. Region prioritization for the development of carbon capture and utilization technologies. *J. CO₂ Util.* 17, 50–59. <https://doi.org/10.1016/j.jcou.2016.10.002>.
- Petak, K., Vidas, H., Manik, J., Palagummi, S., Ciatto, A., Griffith, A., 2017. U.S. Oil and gas infrastructure investment. Through 2035. <https://www.api.org/news-policy-and-issues/energy-infrastructure/oil-gas-infrastructure-study-2017>.
- Peterson, S., 2013. Preliminary geothermal gradient mapping in Alaska's cook inlet forearc basin. *GRC Transation* 37. <https://publications.mygeoenerynow.org/grc/1030587.pdf>.
- Sadiq, J.Z.a.H.M., 2014. Efficiency of geothermal power plants: a worldwide review. *Geothermics* 51, 142–153. <https://doi.org/10.1016/j.geothermics.2013.11.001>.
- Siebels, A., Bults, A., Nolten, M., Wierenga, J., Doust, H., Verbeek, J., 2022. Potential for CO₂ sequestration in saline formations in the western offshore Netherlands: a preliminary study—expanding carbon capture and storage beyond depleted fields. *AAPG (Am. Assoc. Pet. Geol.) Bull.* 106 (9), 1855–1876. <https://doi.org/10.1306/02252221018>.
- Sinha, A., Realff, M.J., 2019. A parametric study of the techno-economics of direct CO₂ air capture systems using solid adsorbents. *AIChE J.* 65 (7), e16607. <https://doi.org/10.1002/aic.16607>.
- Trevino, R.a.M.T., 2019. Offshore CO₂ storage resource assessment of the northern Gulf of Mexico (Texas-Louisiana). place = United States. <https://doi.org/10.2127/1575411>.
- Valentine, J., Zoelle, A., Homsy, S., Mantripragada, H., Woods, M., Roy, N., Fout, T., 2022. Direct air capture case studies. Sorbent System. <https://doi.org/10.2172/1879535>. DOE/NETL-2021/2865.
- Vaught, T.L., 1980. Temperature gradients in a portion of Michigan. A review of the usefulnes of data from the AAPG geothermal survey of North America. <https://www.osti.gov/servlets/purl/5109817>.
- Wang, G., Li, K., Wen, D., Lin, W., Lin, L., Liu, Z., Wang, W., 2013. In: Assessment of geothermal resources in China. Proceedings, 38th Workshop on Geothermal Reservoir Engineering. Stanford University, Stanford, California. February 11–13. SGP-TR-198. <https://pangea.stanford.edu/ERE/pdf/IGAstandard/SGW/2013/Wang.pdf>.
- Wang, G., Zhang, W., Ma, F., Lin, W.-j., Liang, J.-y., Zhu, X., 2018. Overview on hydrothermal and hot dry rock researches in China. *China Geology* 1 (2), 273–285. <https://doi.org/10.31035/cg2018021>.
- Weers, J., Anderson, A., Taverna, N., 2022. The geothermal data repository: ten years of supporting the geothermal industry with open access to geothermal. In: Data Geothermal Rising Conference. Nevada, Reno. <https://www.nrel.gov/docs/fy22osti/82837.pdf>.
- Wiegner, J.F., Grimm, A., Weimann, L., Gazzani, M., 2022. Optimal design and operation of solid sorbent direct air capture processes at varying ambient conditions. *Ind. Eng. Chem. Res.* 61 (34), 12649–12667. <https://doi.org/10.1021/acs.iecr.2c00681>.
- Wurzbacher, J.A., Gebald, C., Brunner, S., Steinfeld, A., 2016. Heat and mass transfer of temperature–vacuum swing desorption for CO₂ capture from air. *Chem. Eng. J.* 283, 1329–1338. <https://doi.org/10.1016/j.cej.2015.08.035>.
- Zafar, D., 2023. An Assessment of Texas' Geothermal Resources and Economic Potential. GSA Annual Meeting & Exposit, Charlotte, 2012. North Carolina. Retrievied on. <https://gsa.confex.com/gsa/2012AM/webprogram/Handout/Paper209399/GSA%20Geothermal%20Texas.pptx>. from.
- Zhu, J., Hu, K., Lu, X., Huang, X., Liu, K., Wu, X., 2015. A review of geothermal energy resources, development, and applications in China: current status and prospects. *Energy* 93, 466–483. <https://doi.org/10.1016/j.energy.2015.08.098>.